

Received February 16, 2022, accepted February 24, 2022, date of publication February 28, 2022, date of current version March 8, 2022.

Digital Object Identifier 10.1109/ACCESS.2022.3155121

Robust Sliding Mode Control-Based a Novel Super-Twisting Disturbance Observer and Fixed-Time State Observer for Slotless-Self Bearing Motor System

QUANG DICH NGUYEN¹, HUY PHUONG NGUYEN², DUC NHAN VO¹, XUAN BIEN NGUYEN^{1,3}, SATOSHI UENO⁴, (Senior Member, IEEE), SHYH-CHOUR HUANG⁵, (Senior Member, IEEE), AND VAN NAM GIAP^{1,2}

¹Institute for Control Engineering and Automation, Hanoi University of Science and Technology, Hai Ba Trung, Hanoi 100000, Vietnam

²School of Electrical Engineering, Hanoi University of Science and Technology, Hai Ba Trung, Hanoi 100000, Vietnam

³Faculty of Mechanical Engineering, Thuyloi University, Dong Da, Hanoi 100000, Vietnam

⁴Department of Mechanical Engineering, Ritsumeikan University, Kusatsu 525-8577, Japan

⁵Department of Mechanical Engineering, National Kaohsiung University of Science and Technology, Kaohsiung 807618, Taiwan

Corresponding author: Van Nam Giap (nam.giapvan@hust.edu.vn)

This work was supported by the Ministry of Education and Training, Vietnam, under Contract CT2020.02.BKA.06.

ABSTRACT The disturbance and uncertainty of the motor drive systems are very complicated terms. There is no exception for the slotless-self bearing motor (SSBM), where the perturbations of the bearing motor are mainly came from the outside as the wind affect, from inside as the thermal changing of the coils, and incorrect modeling of the winding processes. First, to delete these inversed terms, this paper proposes a new super-twisting disturbance observer (STDOb) to obtain the desired goal of the robust control design. The proposed disturbance observer was based on the information of measured and estimated states with the aim of softening the cost of the measurement. Second, to estimate the velocities and accelerations of the movements on x - and y -axes, the stability concept of homogeneous function-based was used to design the fixed-time state observers (FTSOBs) for these axes. The state of the rotational operation on ω - axis was estimated with a fixed-time state observer. Third, to control the positions and rotational speed, a variable boundary layer thickness (VBLT) fixed-time sliding mode control (FTSMC) was designed to force these positions and speed states converge to the desired goals. Finally, the stability of the proposed control algorithm was theoretically verified by using Lyapunov condition and simulation of MATLAB software. The obtained states were acceptably stable with small overshoots, small settling-times, and stable steady-states.

INDEX TERMS Slotless-self bearing motor, super-twisting disturbance observer, variable boundary layer thickness, fixed-time sliding mode control.

I. INTRODUCTION

The concept of interaction between magnetic field and ferri-ferite materials was intelligently used to create the magnetic machines such as bearingless systems, self-bearing motors, levitation devices, etc. The advantages of the magnetic bearing devices are frictionless, non-contact working, no lubrication. The main problem of the bearingless system is how to design the precision control scheme. Some papers presented the control designs for the magnetic devices such as follows:

The associate editor coordinating the review of this manuscript and approving it for publication was Wonhee Kim¹.

The control designs for the active magnetic bearing systems were discussed in [1]–[5]. In this paper, the SSBM control system is presented. The basic concepts of the SSBM can be found in [6]–[10]. Some efforts to reduce the size of bearing systems were presented in [11], [12]. In this paper the robust control algorithms were presented for SSBM system. Due to the limit number of the investigations of the disturbance rejection techniques for SSBM, this paper proposed a new super-twisting disturbance observer to meet the goal of precision control design. Especially, the sources of disturbances and uncertainties of the SSBM were ignored in [8]–[10]. In this paper, all these mentioned terms will be clearly clarified by

each source such as the fabrication process will make huge error of winding process, there are included the distortions of hexagonal shapes of the SSBM, the incorrect of initial angle of the shape, the stacks of the wires, and the incorrect lengths of the shape' edges. These errors are called uncertainties. To manually correct these uncertainties is a difficult task. However, to compensate these disturbance and uncertainty of the SSBM by using the mathematical operation is simpler and more precise. Otherwise, to design the sliding mode control for SSBM system, the first derivative of state vectors are needed. Sometimes, these vector can be obtained by directly taking derivation of the measured output vectors. However, the derivation action leads the obtain information to incorrect terms. To obtain the goal of robust control and avoid the incorrect of the first derivative state vector, the state observer is highly recommended. After obtained the state vectors such as the velocities and accelerations of the movements on three coordinates, the proposed disturbance observer concept was used to design the STDDB.

Basically, disturbance and uncertainty of a physical system are well known as the inversed terms, which usually pull down the performances of a control system. Many papers discussed and proposed the disturbance observers as follows: In [13], the high-order DOB was proposed for the motor system with the condition of the after $k + 1$ times of derivative disturbance is equal to zero, then the estimated disturbance will be converged to the true disturbance value. The disturbance and uncertainty estimation for wind energy convergence system was discussed in [14] with the low-varying uncertainty. The fault estimation with the condition of the boundary condition of first derivative disturbance value was proposed for Takagi-Sugeno fuzzy system [15]. The basic nonlinear disturbance observer (DOB) was proposed in [16]. In [17], the nonlinear DOB was used to estimate the perturbation of the motor control system. The nonlinear DOB for overhead crane system was discussed in [18]. Some developments of nonlinear DOB can be found in [19], [20].

The motivations of this study are mainly divided into three terms: First, the state observer for highly nonlinear such as the SSBM is difficulty requested. In the real application, the fixed-time state observer with the function of switching control helps the observer overcome the proportional nonlinear characteristics in compare with the simple high gain observer. Furthermore, the fixed-time observer only needs the information of the output signal of the physical and estimated systems. The request of the first derivation of the measured signal was deleted. Therefore, the incorrect of derivation of the state vector was not appeared. Second, motivated from the previous papers, there are so complicated conjunction of the disturbance observers such as the first derivative disturbance need to be zero, which mean to the low frequency disturbance can be deleted by these proposed disturbance observers [16], [17]. In our developments of nonlinear disturbance observers in [19]–[21] still need some conjunctions of parameters. Or some disturbance observers just only can be used to estimate the fixed format

of disturbance value such as [22]–[24]. This paper aims to provide a new super-twisting DOB for the SSBM system with simple structure and simple condition. There is only the state observer requested together with the DOB. The conjunctions of fixed format of disturbance value and the first derivative disturbance condition were free. Due to the reason of the condition of the existence of the state observer, the fixed-time state observer was used to estimate the states on the x –, y –, and ω – axes, respectively. Third, to reduce the chattering and overcome the effects of initial condition, this paper proposed a new concept as the variable boundary layer thickness sliding mode control (SMC) for controlling the movements of three axes, respectively. The boundary layer thickness was also considered in the fixed-time SMC. The proposed concept was suitable with the small scale of SSBM. According to the best of author's knowledge, this may the first consideration of the variable boundary layer thickness of fixed-time SMC.

State observers are important soft measurement techniques, which is used to estimate the immeasurable or difficult to be measured terms. There are many state observers such as extended state observer, linear matrix inequality-based state observer, sliding mode observer, etc. The stabilities of these observers are finite-time. Which were strongly affected by the initial conditions. Taking this weaken point as the motivation of the work, the fixed-time state observer was design to estimate the states of the three axes of movement on x –, y –, and rotation of ω – axes, respectively. The states of the movement of the speed coordinate was estimated with a simple fixed-time observer. Otherwise, the states of the movements of x – and y – axes were estimated by the homogeneous function-based state observers. The stability of the homogeneous function-based state observer was provided in [25]. The advantages of the fixed-time observer are listed as simple in design the gains of the observer and free conjunction of the initial condition. After obtained the information of the states and disturbances, the fixed-time controllers with the variable boundary layer thickness were proposed to control the positions and speed, respectively.

Sliding mode control is nonlinear control method, which consists the switching control and equivalent controls. These control values are responsible for forcing the system state converge to the predefined surface and stabilize system state on that surface, respectively [26]. Recently years, the boundary layer thickness with the variability was discussed as in [1] and [27]. In this paper, the fixed-time sliding mode control is improved by using the adaptive saturation function. The basic concept of fixed-time stability can be found in [28]. The applications of the fixed-time concept can be found in [29]–[32]. The number of investigations of the flexible boundary layer thickness of fixed-time stability are still limited. Therefore, this paper proposed a new design of fixed-time stability especially for small system. The main contributions and originalities of this paper are listed as follows:

1. The fully descriptions of the embedded external and internal perturbations of the SSBM were clearly

presented in this paper, which were not appeared in the previous works [8]–[10]. The efforts of the modeling is aimed to softening the control design processes. The correct mathematical model of the SSBM helps the control performances become better. Therefore, this paper carefully presented the sources of perturbations of SSBM. Which is a helpful step for considering the robust control of a motor system.

2. The homogeneous stability-based state observer was used to design the states observers for SSBM, where the velocities, accelerations of the movement on x –, y – axes can be easily obtained. Otherwise, the state of the rotation of ω – axis was estimated by the fixed-time state observer. These states are costly known by using physical sensors. The estimation design used the position sensors, and encoder only. This effort is aimed to reduce the cost of the product and improve the precision of the control design. The derivation procedure of position to get velocity and acceleration processes was completely removed.
3. In this paper, a new super-twisting DOB was proposed to design the disturbance observer for SSBM system. The proposed DOB can work with the information of estimated and measured signals. Furthermore, the DOB in this paper can estimate disturbances at both low and high frequencies. This means that the first derivative disturbance is here free. Furthermore, there is no condition of the high order derivation of disturbance equal to zero. The originality of the proposed DOB is figured out that there is no conjunction of the first derivative disturbance such as the DOB in [16]–[18]. The proposed DOB can estimate perturbations in many different formats. There is no need the prior format of the perturbations such as [22]–[24]. This is a huge suggestion for future direction of the area of disturbance rejection control design.
4. A novel boundary layer thickness of FTSMC is presented in this paper to control the positions and speed of the SSBM system. This is new concept of an improved fixed-time stability in compare with our previous paper [21]. Finally, the proposed method was theoretically verified by using the Lyapunov condition. The correction and effectiveness of the proposed methods were theoretically verified by Lyapunov condition and the simulation in MATLAB software.

The structure of this paper is as follows: First, the introduction of the SSBM and some related concepts of the proposed control algorithms were given in the first section of the paper. In the second section, the mathematical model of the SSBM with fully sources of disturbances and uncertainties is presented together with some preliminary mathematics. In the third section, the proposed methods are given for SSBM system, respectively. In the fourth section, the performances of the proposed methods for SSBM is given. Finally, the conclusion of the work is given in the last section with some comments of the future work.

Notes: The vector symbols are bolds and italics. Matrix is bold capital. x_r, x_m and \hat{x} are used to represent the algebra values of referenced, measured, and estimated signals, respectively. $|\bullet|$ is the absolute value. $sign(\mathbf{x}^T) = [sign(x_1), sign(x_2), \dots, sign(x_n)]^T$. $sign(x_i) = 1$ if $x_i > 0$, $sign(x_i) = -1$ if $x_i < 0$, and $sign(x_i) = 0$ if $x_i = 0$. $sat(s/\varepsilon) = 1$ if $s > \varepsilon$, $sat(s/\varepsilon) = -1$ if $s < -\varepsilon$, and $sat(s/\varepsilon) = s/\varepsilon$ if $s \in (-\varepsilon, \varepsilon)$. $\mathbf{x}^T = [x_1, x_2, \dots, x_n]^T$. $\int \bullet$ is integral respect to the time, which is used to represent the calculation of $\int_0^t d(\tau)$.

II. MATHEMATICAL MODEL OF SSBM AND SOME PRELIMINARY MATHEMATICS

This section presents the mathematical model of the SSBM and some related mathematics of the utilized control methods. Details are given in the subsections below.

A. MATHEMATICAL MODEL OF THE SSBM

Our proposed bearing motor was clearly presented in [10]. The motor was made by the combination of a cylindrical, two poles of permanent magnet block, a back yoke, a shaft, and one term fixed these components as a fixed block. The stator is fabricated without the iron core with six phases. The mathematical model analysis can be found in [10]. The structure of the SSBM can be redrawn as in Fig. 1 below. The design of SSBM was presented in [10]. The winding coils of the stator was designed as a hexagonal shapes. In the winding process, the errors were appeared from the winding distortions. There are angle of the hexagonal shape, the initial angular positions of the coils, and the incorrect lengths of the shapes' edge.

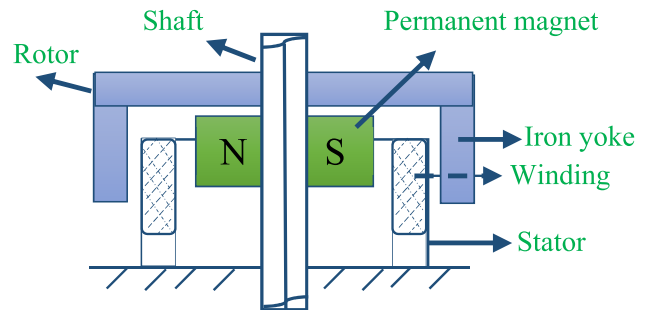


FIGURE 1. Structure of SSBM.

The angular positions of the parallel parts were calculated as below.

$$\begin{cases} \theta_{+phase}^k = (\theta_0 + \Delta\theta_{+phase}^k) + \frac{k-1}{3n}\pi + \frac{2m}{6}\pi \\ \theta_{-phase}^k = (\theta_0 + \Delta\theta_{-phase}^k) + \frac{k-1}{3n}\pi + \frac{2m+3}{6}\pi \end{cases} \quad (1)$$

where θ_{+phase}^k and θ_{-phase}^k are angular position for parallel turns with number k . Total of the turns is n , the phase is referred by m , the number of turn is k . The angular position of +a-phase is θ_0 . k was selected as an odd number to avoid the overlap. $\Delta\theta_{+phase}^k$ and $\Delta\theta_{-phase}^k$ are errors of the angular

positions for each phase. The positions of the shapes need to be made within small errors to satisfy the constraints of the flux-density, magnetic field, and the relations of the forces and torque in SSBM. The errors of the angular positions need to be bounded as the assumption 1 below.

Assumption 1: The uncertainties of the angular positions should be bounded as follows: $|\Delta\theta_{+phase}^k| \leq \xi_{\theta+}^k$ and $|\Delta\theta_{-phase}^k| \leq \xi_{\theta-}^k$ where $\xi_{\theta+}^k$ and $\xi_{\theta-}^k$ need to be positively defined.

The magnetic field is

$$\mathbf{B}_{ag} = (B + \Delta B) \cos((\theta + \Delta\theta) - \psi) \quad (2)$$

where B is the magnitude of magnetic flux density. The angular position of the rotor is ψ . $\Delta\theta$ is winding error of angular position. ΔB is uncertainty of magnetic field, which comes from the length of the wire. Eq. (2) can be rewritten as follows:

$$\mathbf{B}_{ag} = B \cos(\theta - \psi) + \Delta\mathbf{B}_{ag} \quad (3)$$

The magnetic field error is mainly effected by the permeability of the environment and the length of the edge' shapes. The reference permeability is vacuum environment. However in the real working condition, there is some small error. Furthermore, the referenced lengths for edges of the hexagonal shapes are generally defined. In the winding process, these lengths are sometimes incorrect. These error of permeability and the shapes' edge need to be bounded. The system can work if the uncertainty $\Delta\mathbf{B}_{ag}$ is bounded as the assumption 2 below.

Assumption 2: The uncertainty of magnetic field need to be bounded as follows: $|\Delta\mathbf{B}_{ag}| \leq \mathbf{B}_{max}$, where \mathbf{B}_{max} is positively defined.

In the previous paper [10], the Lorentz forces were calculated as follows: $F_{+a}^f = F_{+d}^f, F_{-a}^f = F_{-d}^f, F_{+b}^f = F_{+e}^f, F_{-b}^f = F_{-e}^f, F_{+c}^f = F_{+f}^f, F_{-c}^f = F_{-f}^f$. Due to the winding errors, these forces of the phases were not equal. The magnitudes of forces of the phases a and d can be calculated as follows:

$$\begin{cases} F_{+a}^f = |Bl i_a^f \cos(\theta_0 - \psi)| + \Delta F_{+a}^f \\ F_{+d}^f = |Bl i_a^f \cos(\theta_0 - \psi)| + \Delta F_{+d}^f \\ F_{-a}^f = |Bl i_a^f \sin(\theta_0 - \psi)| + \Delta F_{-a}^f \\ F_{-d}^f = |Bl i_a^f \sin(\theta_0 - \psi)| + \Delta F_{-d}^f \end{cases} \quad (4)$$

$\Delta F_{+a}^f, \Delta F_{-a}^f, \Delta F_{+d}^f$, and ΔF_{-d}^f are the uncertainties of the forces of fabrication errors from the angular position errors and the errors of the length of wires. Herein, l is used to describe the nominal length of the wire, i_a^f is current of generated the bearing force of a -phase. The unwanted imprecision of forces are mainly came from the magnetic field, lengths of shape' edges, and the imperfection of the angular position for each shape. To obtain the expected force, these uncertainties need to be bounded as the assumption 3 below.

Assumption 3: The uncertainties of forces are bounded as follows: $|\Delta F_{+a}^f| \leq \xi_{F+a}^f, |\Delta F_{-a}^f| \leq \xi_{F-a}^f, |\Delta F_{+d}^f| \leq \xi_{F+d}^f$ and $|\Delta F_{-d}^f| \leq \xi_{F-d}^f$, where these $\xi_{F+a}^f, \xi_{F-a}^f, \xi_{F+d}^f, \xi_{F-d}^f$ are positively defined.

The amplitudes Lorentz forces on for phase a-d, b-e, and c-f are calculated as follows:

$$\begin{cases} F_a = \sqrt{(F_{+a}^f + F_{+d}^f)^2 + (F_{-a}^f + F_{-d}^f)^2} \\ F_b = \sqrt{(F_{+b}^f + F_{+e}^f)^2 + (F_{-b}^f + F_{-e}^f)^2} \\ F_c = \sqrt{(F_{+c}^f + F_{+f}^f)^2 + (F_{-c}^f + F_{-f}^f)^2} \end{cases} \quad (5)$$

where F_a , Eq. (5) should be changed as below.

$$\begin{cases} F_a = 2Bl i_a^f + \Delta F_a \\ F_b = 2Bl i_b^f + \Delta F_b \\ F_c = 2Bl i_c^f + \Delta F_c \end{cases} \quad (6)$$

where i_b^f and i_c^f are current of generated the bearing forces of b - and c -phases. $\Delta F_a, \Delta F_b$, and ΔF_c are uncertain forces on a -, b -, c -axes, respectively. The incorrect force for each phase should not exceed a certain value to help the SSBM system can work normally. Other words, the uncertainties of the Lorentz forces need to be bounded as the assumption 4 below.

Assumption 4: The uncertainties of the forces should be bounded as follows: $|\Delta F_a| \leq \xi_{Fa max}, |\Delta F_b| \leq \xi_{Fb max}$, and $|\Delta F_c| \leq \xi_{Fc max}$, where $\xi_{Fa max}, \xi_{Fb max}$, and $\xi_{Fc max}$ should be positively defined.

In [10], the total forces need to be zero as follows:

$$\mathbf{F}_a + \mathbf{F}_b + \mathbf{F}_c = 0 \quad (7)$$

where total force can be calculated as follows:

$$2Bl i_a^f + \Delta F_a + 2Bl i_b^f + \Delta F_b + 2Bl i_c^f + \Delta F_c = 0 \quad (8)$$

The total current is then defined as follows:

$$i_a^f + i_b^f + i_c^f = -\frac{\Delta F_a + \Delta F_b + \Delta F_c}{2Bl} \quad (9)$$

Remark 1: To consider the total current of i_a^f, i_b^f , and i_c^f is to be zero, which was ignored in [10]. These uncertain values in the right hand side of Eq. 9 should be deleted.

Bearing currents are calculated as follows:

$$\begin{cases} i_{a,d}^f = i_d \cos(\psi) + i_q \sin(\psi) + \Delta i_{a,d}^f \\ i_{b,e}^f = i_d \cos(\psi - 2\pi/3) + i_q \sin(\psi - 2\pi/3) + \Delta i_{b,e}^f \\ i_{c,f}^f = i_d \cos(\psi - 4\pi/3) + i_q \sin(\psi - 4\pi/3) + \Delta i_{c,f}^f \end{cases} \quad (10)$$

where i_d is direct current and i_q quadrature current. In [10], the ψ is angular of rotor center in first portion of the circle with the x -axis. This angular sometime is not nominal, which is main reason of uncertainties for bearing currents. For motor can start and work normally, the rotor should be located in a suitable area. Therefore, uncertainties of the bearing currents need to be bounded as the assumption 5 below.

Assumption 5: The uncertainties of the bearing currents need to fulfil $|\Delta i_{a,d}^f| \leq \xi_{iad}^f \max$, $|\Delta i_{b,e}^f| \leq \xi_{ibe}^f \max$, and $|\Delta i_{c,f}^f| \leq \xi_{icf}^f \max$, where $\xi_{iad}^f \max$, $\xi_{ibe}^f \max$, and $\xi_{icf}^f \max$ are positively defined.

The torques for three phases are calculated as follows:

$$\begin{cases} \tau_a = B l_a^T (\cos(\theta_0 - \psi) + \sin(\theta_0 - \psi)) R + \Delta \tau_a \\ \tau_b = B l_b^T (\cos(\theta_0 + \frac{\pi}{3} - \psi) + \sin(\theta_0 + \frac{\pi}{3} - \psi)) R + \Delta \tau_b \\ \tau_c = B l_c^T (\cos(\theta_0 + 2\frac{\pi}{3} - \psi) + \sin(\theta_0 + 2\frac{\pi}{3} - \psi)) R + \Delta \tau_c \end{cases} \quad (11)$$

where R is the radius of the rotor. The sources of the uncertainties of the torques from the length of shape' edges errors, errors of the angular positions of the shape, error angular position of the rotor. These values need to be bounded as follows:

Assumption 6: The uncertainties of torques should be bounded as follows: $|\Delta \tau_a| < \xi_{\tau a} \max$, $|\Delta \tau_b| < \xi_{\tau b} \max$, and $|\Delta \tau_c| < \xi_{\tau c} \max$, where $\xi_{\tau a} \max$, $\xi_{\tau b} \max$, and $\xi_{\tau c} \max$ are positively defined.

The motor currents are calculated as follows:

$$\begin{cases} i_{a,d}^T = \pm A_m \cos(\phi_m) + \Delta i_{a,d}^T \\ i_{b,e}^T = \pm A_m \cos(\phi_m + \pi/3) + \Delta i_{b,e}^T \\ i_{c,f}^T = \pm A_m \cos(\phi_m + 2\pi/3) + \Delta i_{c,f}^T \end{cases} \quad (12)$$

where A_m is amplitude of the motor current. $\Delta i_{a,d}^T$, $\Delta i_{b,e}^T$, and $\Delta i_{c,f}^T$ are transposed uncertainties of the currents. These error also must be bounded. The currents of the opposite phases are calculated as below.

$$\begin{cases} i_{a,d} = i_d \cos(\psi) + i_q \sin(\psi) \pm A_m \cos(\phi_m) + \Delta i_{a,d} \\ i_{b,e} = i_d \cos(\psi - 2\frac{\pi}{3}) + i_q \sin(\psi - 2\frac{\pi}{3}) \\ \quad \pm A_m \cos(\phi_m + \frac{\pi}{3}) + \Delta i_{b,e} \\ i_{c,f} = i_d \cos(\psi - 4\frac{\pi}{3}) + i_q \sin(\psi - 4\frac{\pi}{3}) \\ \quad \pm A_m \cos(\phi_m + 2\frac{\pi}{3}) + \Delta i_{c,f} \end{cases} \quad (13)$$

$\Delta i_{a,d}$, $\Delta i_{b,e}$, and $\Delta i_{c,f}$ are uncertainties of the currents. The torques and forces finally can be calculated as follows:

$$\begin{cases} \tau = k_{nm} k_m A \sin(\phi_m - \psi + \theta_0 + \frac{\pi}{4}) + \Delta \tau \\ f_x = -k_{nb} k_b \{i_d \sin(2\theta_0) - i_q \cos(2\theta_0)\} + \Delta f_x \\ f_y = k_{nb} k_b \{i_d \cos(2\theta_0) + i_q \sin(2\theta_0)\} + \Delta f_y \end{cases} \quad (14)$$

where τ is torque of the motor, f_x and f_y is the force on x-axis, and y-axis, respectively. $\Delta \tau$, Δf_x , and Δf_y are the uncertainties of the motor system. These uncertainties also need to be

bounded. Some parameters are calculated as follows:

$$\begin{cases} k_m = -(3\sqrt{2} l_p + \frac{8(6 - 3\sqrt{2})}{\pi} l_l) r B + \Delta k_m \\ k_b = -(3 l_p + \frac{12}{\pi} l_l) B + \Delta k_b \\ k_{nm} = 1 + 2 \cos(\frac{\pi}{3n}) + 2 \cos(2\frac{\pi}{3n}) + \dots + 2 \cos(\frac{n-1}{2} \frac{\pi}{3n}) \\ \quad + \Delta k_{nm} \\ k_{nb} = 1 + 2 \cos(2\frac{\pi}{3n}) + 2 \cos(4\frac{\pi}{3n}) + \dots + 2 \cos((n-1) \frac{\pi}{3n}) \\ \quad + \Delta k_{nb} \end{cases} \quad (15)$$

where l_p and l_l are parallel and projection length, respectively. The radius winding is r . Δk_m , Δk_b , Δk_{nm} , and Δk_{nb} are the uncertainties of winding process. The torque and forces with fully embedded disturbances and uncertainties are calculated as follows:

$$\begin{cases} \tau = k_{nm} k_m A_m + \Delta \tau + d_\tau \\ F_x = k_{nb} k_b i_q + \Delta F_x + d_{F_x} \\ F_y = k_{nb} k_b i_d + \Delta F_y + d_{F_y} \end{cases} \quad (16)$$

Eq. (16) can be simplified as follows:

$$\begin{cases} \tau - T_l = J \dot{\omega} \\ F_x - F_{lx} = m \ddot{x} \\ F_y - F_{ly} = m \ddot{y} \end{cases} \quad (17)$$

where $T_l = \Delta \tau + d_\tau$, $F_{lx} = \Delta F_x + d_{F_x}$, and $F_{ly} = \Delta F_y + d_{F_y}$. Where F_{lx} , F_{ly} , and T_l are perturbations on the x -, y -, and ω -axes, respectively. E.q (17) can be simply rewritten by using the magnitude value as follows:

$$\begin{cases} \frac{k_{nm} k_m A_m}{J} - \frac{T_l}{J} = \dot{\omega} \\ \frac{k_{nb} k_b i_q}{m} - \frac{F_{lx}}{m} = \ddot{x} \\ \frac{k_{nb} k_b i_d}{m} - \frac{F_{ly}}{m} = \ddot{y} \end{cases} \quad (18)$$

The imperfections of the fabrication were mentioned above together with the outside effects such as self-vibration of the rotor with the working platform and wind effect on the rotor of SSBM should be calculated as a unique term for each coordinate. The SSBM can work if the perturbations of the system are bounded as the assumption 7 below.

Assumption 7: The disturbances on three axes need to be limited as follows: $|T_l| < \gamma_T$, $|F_{lx}| < \gamma_{F_x}$, and $|F_{ly}| < \gamma_{F_y}$, where γ_T , γ_{F_x} and γ_{F_y} are positively constant defined.

B. PRELIMINARY MATHEMATICS

In this paper, the fixed-time observer concept was used to design the state observer for the speed coordinate and homogeneous function-based FTSOB in [25] was used to design the state observer for the movements of x - and y - axes, respectively. These efforts aimed to obtain the system states

without the effect of the nonlinear and the incorrect of first derivative state. First, the generalized system as

$$\begin{cases} \dot{x}_1 = x_2 \\ \dot{x}_2 = bu + cd \end{cases} \quad (19)$$

is considered. The proposed state observer is as follows:

$$\begin{cases} \dot{\hat{x}}_1 = \hat{x}_2 + k_1 |x_1 - \hat{x}_1|^{\alpha_1} \text{sign}(x_1 - \hat{x}_1) \\ \dot{\hat{x}}_2 = bu + c\hat{d} + k_2 |x_1 - \hat{x}_1|^{\alpha_2} \text{sign}(x_1 - \hat{x}_1) \end{cases} \quad (20)$$

Using Eq. (19) to subtract for Eq. (20) yields

$$\begin{cases} \dot{e}_1 = e_2 - k_1 |x_1 - \hat{x}_1|^{\alpha_1} \text{sign}(x_1 - \hat{x}_1) \\ \dot{e}_2 = c\tilde{d} - k_2 |x_1 - \hat{x}_1|^{\alpha_2} \text{sign}(x_1 - \hat{x}_1) \end{cases} \quad (21)$$

where $e_1 = x_1 - \hat{x}_1$, $e_2 = x_2 - \hat{x}_2$, and $\tilde{d} = d - \hat{d}$. For simple in design the state observer, the disturbance error was assumed equal to zero. The Eq. (21) is then can be rewritten as follows:

$$\begin{cases} \dot{e}_1 = e_2 - k_1 |x_1 - \hat{x}_1|^{\alpha_1} \text{sign}(x_1 - \hat{x}_1) \\ \dot{e}_2 = -k_2 |x_1 - \hat{x}_1|^{\alpha_2} \text{sign}(x_1 - \hat{x}_1) \end{cases} \quad (22)$$

According to the paper [25], the parameters should be selected as follows $\alpha_1 \in (1 - \varepsilon, 1)$, $\varepsilon > 0$, $\alpha_2 = 2\alpha_1 - (2 - 1) = 2\alpha_1$, and $\mathbf{A} = \begin{bmatrix} -k_1 & 1 \\ -k_2 & 0 \end{bmatrix}$ is Hurwitz. To prove the fixed-time stability, the stable for system as follows:

$$\dot{e} = \mathbf{K}e \quad (23)$$

is analyzed. Eq. (23) is stable if \mathbf{K} is Hurwitz. The Lyapunov is then should be $V(e) = e^T \mathbf{P}e$. Therefore,

$$\begin{aligned} \dot{V}(e) &= \dot{e}^T \mathbf{P}e + e^T \mathbf{P}\dot{e} \\ &= e^T (\mathbf{K}^T \mathbf{P} + \mathbf{P}\mathbf{K})e \end{aligned} \quad (24)$$

The matrix \mathbf{K} is requested to satisfy

$$\mathbf{K}^T \mathbf{P} + \mathbf{P}\mathbf{K} = -\mathbf{Q} \quad (25)$$

where \mathbf{Q} is positively defined. Eq. (24) is then negatively defined. If $\xi = [e^{1/r_1}, e^{1/r_2}, \dots, e^{1/r_n}]$, $V(\xi) = \xi^T \mathbf{P}\xi$. If Eq. (24) is obtained leads to $\dot{V}(\xi) < 0$. $V(\xi)$ is then called homogeneous stability. If $n = \alpha - 1$, with $0 < \alpha < 1$, therefore $V(\xi) \leq \lambda_{\max}(\mathbf{P}) \|e\|^2$ and

$$\dot{V}(\xi) \leq -\lambda_{\min}(\mathbf{Q}) \|e\|^2 \quad (26)$$

or

$$\dot{V}(\xi) \leq -\frac{\lambda_{\min}(\mathbf{Q})}{\lambda_{\max}(\mathbf{P})} V^{1+n}(\xi) \quad (27)$$

Integrating both sides of Eq. (27) yields

$$\int_{V(0)}^{V(\infty)} d(V(\xi)) V^{-1-n}(\xi) \leq -\frac{\lambda_{\min}(\mathbf{Q})}{\lambda_{\max}(\mathbf{P})} \int_0^{T_{\max}} dt \quad (28)$$

or

$$\frac{1}{n} V^{-n}(\xi(0)) \geq \frac{\lambda_{\min}(\mathbf{Q})}{\lambda_{\max}(\mathbf{P})} T_{\max} \quad (29)$$

or

$$\begin{aligned} T_{\max} &\leq \frac{\lambda_{\max}(\mathbf{P})}{\lambda_{\min}(\mathbf{Q})} \frac{1}{n} V^{1-\alpha}(\xi(0)) \\ &\leq \frac{\lambda_{\max}^{2-\alpha}(\mathbf{P})}{\lambda_{\min}(\mathbf{Q})} \frac{1}{n} \end{aligned} \quad (30)$$

The estimation errors are then fixed-time stable.

Remark 2: The gains of fixed-time observer in Eq. (20) should be approximately chosen to avoid the chattering phenomenon.

After obtained the estimated system states, a new disturbance observer was proposed as follows:

$$\begin{aligned} \hat{d} &= \frac{1}{c}(bu + c\hat{d} + k_2 |x_1 - \hat{x}_1|^{\alpha_2} \text{sign}(x_1 - \hat{x}_1) - bu) \\ &\quad + k_{d1} \int \left| \frac{1}{c}(bu + k_2 |x_1 - \hat{x}_1|^{\alpha_2} \text{sign}(x_1 - \hat{x}_1) - bu) \right|^{1/2} \\ &\quad \times \text{sign}\left(\frac{1}{c}(bu + k_2 |x_1 - \hat{x}_1|^{\alpha_2} \text{sign}(x_1 - \hat{x}_1) - bu)\right) \\ &\quad + k_{d2} \iint \text{sign}\left(\frac{1}{c}(bu + k_2 |x_1 - \hat{x}_1|^{\alpha_2} \text{sign}(x_1 - \hat{x}_1) - bu)\right) \end{aligned} \quad (31)$$

where \hat{d} is estimated of d .

Remark 3: The integral in Eq. (31) is corresponded to the time (t) and its derivative is defined by $\frac{d}{dt} \int_0^t f(t) dt = f(t)$.

Since

$$\begin{aligned} &\frac{1}{c}(bu + c\hat{d} + k_2 |x_1 - \hat{x}_1|^{\alpha_2} \text{sign}(x_1 - \hat{x}_1) - bu) \\ &= \frac{1}{c}(\hat{x}_2 + cd - \dot{x}_2) \\ &= \tilde{d} \end{aligned} \quad (32)$$

and

$$\begin{aligned} &\frac{1}{c}(bu + k_2 |x_1 - \hat{x}_1|^{\alpha_2} \text{sign}(x_1 - \hat{x}_1) - bu) \\ &= \frac{1}{c}(\hat{x}_2 - c\hat{d} + cd - \dot{x}_2) \\ &= \tilde{d} \end{aligned} \quad (33)$$

where $d - \hat{d} = \tilde{d}$. Eq. (31) can be rewritten as follows:

$$\hat{d} = d + k_{d1} \int |\tilde{d}|^{1/2} \text{sign}(\tilde{d}) + k_{d2} \iint \text{sign}(\tilde{d}) \quad (34)$$

Taking derivative for both side of Eq. (34) yields

$$\dot{\hat{d}} = \dot{d} + k_{d1} |\tilde{d}|^{1/2} \text{sign}(\tilde{d}) + k_{d2} \int \text{sign}(\tilde{d}) \quad (35)$$

or

$$\dot{\tilde{d}} = -k_{d1} |\tilde{d}|^{1/2} \text{sign}(\tilde{d}) - k_{d2} \int \text{sign}(\tilde{d}) \quad (36)$$

Remark 4: The format of the proposed disturbance observer in Eq. (36) is called super-twisting disturbance observer.

The Lyapunov condition for stability analysis of disturbance observer can be chosen as follows:

$$V(d) = \frac{1}{2} \tilde{d}^2 \tag{37}$$

Taking derivative for both sides of Eq. (37) yields

$$\dot{V}(d) = \tilde{d} \dot{\tilde{d}} \tag{38}$$

Using Eq. (36) to solve Eq. (38) leads to

$$\begin{aligned} \dot{V}(d) &= -k_{d1} |\tilde{d}|^{1/2} \tilde{d} \text{sign}(\tilde{d}) - k_{d2} \tilde{d} \int \text{sign}(\tilde{d}) \\ &\leq -k_{d1} |\tilde{d}|^{1/2} |\tilde{d}| - |\tilde{d}| \int k_{d2} \end{aligned} \tag{39}$$

with k_{d1} and k_{d2} are positively defined, Eq. (39) become negatively defined.

This completes the proof of stability for the proposed STDOB.

In this paper, a new variable boundary layer thickness FTSMC was designed to control the positions on x -, y -, and rotational speed on ω -axes, respectively. The fixed-time function is generally described as follows:

$$\dot{s} = -\gamma_1 |s|^{\frac{\kappa_1}{\eta_1}} \text{sat}\left(\frac{s}{\phi} - k_0 \int s\right) - \gamma_2 |s|^{\frac{\kappa_2}{\eta_2}} \text{sat}\left(\frac{s}{\phi} - k_0 \int s\right) \tag{40}$$

where γ_1 and γ_2 and k_0 should be positively defined. ϕ is boundary layer of the fixed saturation function. The condition of $\kappa_1 > \eta_1$, and $\kappa_2 < \eta_2$ should be fulfilled. k_0 need to be suitably chosen to guarantee the value of the saturation function get into the area of $(-\phi, \phi)$. Eq. (40) is satisfied as follows:

$$\dot{s} \leq -\gamma_1 |s|^{\frac{\kappa_1}{\eta_1}} \text{sign}(s) - \gamma_2 |s|^{\frac{\kappa_2}{\eta_2}} \text{sign}(s) \tag{41}$$

According to the previous published paper [28], when the sliding mode surface with the initial condition out of $(-\phi, \phi)$, the settling-time can be calculated as follows:

$$T_{s(out)max} \leq \frac{1}{\gamma_1} \frac{\eta_1}{\kappa_1 - \eta_1} + \frac{1}{\gamma_2} \frac{\eta_2}{\eta_2 - \kappa_2} \tag{42}$$

If the initial condition of sliding mode surface is in $(-\phi, \phi)$, the settling time will be fixed-time in

$$T_{s(in)max} \leq \frac{1}{\gamma_1 + \gamma_2} \tag{43}$$

Proof of stability when $s(0) \in (-\phi, \phi)$.

Eq. (43) can be simplified as follows:

$$\dot{s} \leq -\gamma_1 - \gamma_2 \tag{44}$$

Taking integration for both sides of Eq. (44) respect to the time from zero to infinity yields

$$\int_{s(0)}^{s(\infty)} \dot{s}(t) \leq \int_0^{Tmax} -\lambda_1 - \lambda_2 \tag{45}$$

or

$$s(\infty) - s(0) \leq (-\lambda_1 - \lambda_2)T_{max} \tag{46}$$

or

$$T_{max} \leq \frac{1}{\lambda_1 + \lambda_2} \tag{47}$$

This completes the proof.

Remark 5: The proposed fixed-time stability is suitable for both small and big scale systems. However, the proposed theory is simpler for the small devices.

Remark 6: The proposed control algorithms have ability to reject the disturbances, uncertainties, and unknown nonlinear terms. Furthermore, the settling-time was obtained with fixed-time stability, the chattering was also reduced by using the variable boundary layer thickness of SMC.

The details of proposed control algorithms for the SSBM are shown in the next following section.

III. PROPOSED APPROACH

In this section, the state observers, disturbance observers, and the novel FTSMC designs for SSBM are all given in detail. The organization of this section is as follows: First, the designs of state observers for movements of x - and y -axes and rotational speed are introduced. Second, the disturbance observer based on the information of the estimated and measured states are presented. Third, the novel FTSMC designs for these movements and rotation control systems are introduced. Final, the stability of the whole control system is given to verify the correction of the proposed control methods.

A. THE STATE OBSERVER FOR THE SSBM SYSTEM

1) STATE OBSERVER FOR SPEED COORDINATE

First, the state observer for speed coordinate was designed as follows:

$$\begin{aligned} \dot{\hat{\omega}} &= \frac{k_{nm} k_m A_m}{J} - \frac{\hat{T}_l}{J} + k_{1\omega} |e_\omega|^{\frac{\alpha_{1\omega}}{\beta_{1\omega}}} \text{sign}(e_\omega) \\ &\quad + k_{2\omega} |e_\omega|^{\frac{\alpha_{2\omega}}{\beta_{2\omega}}} \text{sign}(e_\omega) \end{aligned} \tag{48}$$

where $\alpha_{1\omega} > \beta_{1\omega}$, $\alpha_{2\omega} < \beta_{2\omega}$, $k_{1\omega} > 0$, $k_{2\omega} > 0$, and $e_\omega = \omega - \hat{\omega}$. Using the speed equation in Eq. (18) to subtract for both sides of Eq. (48) leads to

$$\dot{e}_\omega = -\frac{\tilde{T}_l}{J} - k_{1\omega} |e_\omega|^{\frac{\alpha_{1\omega}}{\beta_{1\omega}}} \text{sign}(e_\omega) - k_{2\omega} |e_\omega|^{\frac{\alpha_{2\omega}}{\beta_{2\omega}}} \text{sign}(e_\omega) \tag{49}$$

For easy to design the control gains of the state observer such as Eq. (49), the disturbance error should be assumed equal to zero. Therefore, Eq. (49) is then fulfilled the condition of fixed-time stability as Eq. (41). If the Lyapunov for estimation of speed axis is selected as $V(e_\omega) = 0.5e_\omega^2$, then the first derivative $\dot{V}(e_\omega) < 0$. The settling-time of the estimation error is calculated as follows:

$$T_{e_\omega} = \frac{1}{k_{1\omega}} \frac{\beta_{1\omega}}{\alpha_{1\omega} - \beta_{1\omega}} + \frac{1}{k_{2\omega}} \frac{\beta_{2\omega}}{\beta_{2\omega} - \alpha_{2\omega}} \tag{50}$$

The state observers for movement on x - and y -axes are shown in next section below.

2) STATE OBSERVER FOR MOVEMENT OF X-AXIS

First, the mathematical model of the movement on the x -axis is converted into the format as follows:

$$\begin{cases} x_1 = x_2 \\ \dot{x}_2 = \ddot{x} = \frac{k_{nb}k_b i_q}{m} - \frac{F_{lx}}{m} \end{cases} \quad (51)$$

The proposed state observer is as follows:

$$\begin{cases} \dot{\hat{x}}_1 = \hat{x}_2 + k_{1x} |x_1 - \hat{x}_1|^{\alpha_{1x}} \text{sign}(x_1 - \hat{x}_1) \\ \dot{\hat{x}}_2 = \frac{k_{nb}k_b i_q}{m} - \frac{\hat{F}_{lx}}{m} + k_{2x} |x_1 - \hat{x}_1|^{\alpha_{2x}} \text{sign}(x_1 - \hat{x}_1) \end{cases} \quad (52)$$

Using Eq. (51) subtract to Eq. (52) leads to

$$\begin{cases} \dot{e}_{1x} = e_{2x} - k_{1x} |x_1 - \hat{x}_1|^{\alpha_{1x}} \text{sign}(x_1 - \hat{x}_1) \\ \dot{e}_{2x} = -\frac{\tilde{F}_{lx}}{m} - k_{2x} |x_1 - \hat{x}_1|^{\alpha_{2x}} \text{sign}(x_1 - \hat{x}_1) \end{cases} \quad (53)$$

The disturbance error should be assumed equal to zero. As mentioned above, the parameter should be selected as follows: $\alpha_{1x} \in (1 - \varepsilon_x, 1)$, $\varepsilon_x > 0$, $\alpha_{2x} = 2\alpha_{1x} - (2 - 1)$, and $\mathbf{A}_x = \begin{bmatrix} -k_{1x} & 1 \\ -k_{2x} & 0 \end{bmatrix}$ is Hurwitz. According to the previous paper [25], with the $\mathbf{e}_{\bar{x}} = [e_{1x} \ e_{2x}]^T$, the Lyapunov for state estimation of x -axis should be $V(\mathbf{e}_{\bar{x}}) = \mathbf{e}_{\bar{x}}^T \mathbf{P} \mathbf{e}_{\bar{x}}$. Therefore $\dot{V}(\mathbf{e}_{\bar{x}}) < 0$. The settling-time estimation error will be fixed-time stable. Similarly, the state observer of y -axes is designed as follows:

3) STATE OBSERVER FOR MOVEMENT OF Y-AXIS

The mathematical model of the movement on the y -axis also need to be converted into the format as follows:

$$\begin{cases} y_1 = y_2 \\ \dot{y}_2 = \ddot{y} = \frac{k_{nb}k_b i_d}{m} - \frac{F_{ly}}{m} \end{cases} \quad (54)$$

The proposed state observer for y -axis is as follows:

$$\begin{cases} \dot{\hat{y}}_1 = \hat{y}_2 + k_{1y} |y_1 - \hat{y}_1|^{\alpha_{1y}} \text{sign}(y_1 - \hat{y}_1) \\ \dot{\hat{y}}_2 = \frac{k_{nb}k_b i_d}{m} - \frac{\hat{F}_{ly}}{m} + k_{2y} |y_1 - \hat{y}_1|^{\alpha_{2y}} \text{sign}(y_1 - \hat{y}_1) \end{cases} \quad (55)$$

Using Eq. (54) subtract to Eq. (55) leads to

$$\begin{cases} \dot{e}_{1y} = e_{2y} - k_{1y} |y_1 - \hat{y}_1|^{\alpha_{1y}} \text{sign}(y_1 - \hat{y}_1) \\ \dot{e}_{2y} = -\frac{\tilde{F}_{ly}}{m} - k_{2y} |y_1 - \hat{y}_1|^{\alpha_{2y}} \text{sign}(y_1 - \hat{y}_1) \end{cases} \quad (56)$$

The disturbance error also should be assumed equal to zero. Similarly, the parameter should be selected as follows: $\alpha_{1y} \in (1 - \varepsilon_y, 1)$, $\varepsilon_y > 0$, $\alpha_{2y} = 2\alpha_{1y} - (2 - 1)$, and $\mathbf{A}_y = \begin{bmatrix} -k_{1y} & 1 \\ -k_{2y} & 0 \end{bmatrix}$ is Hurwitz. with the $\mathbf{e}_{\bar{y}} = [e_{1y} \ e_{2y}]^T$, the Lyapunov for state estimation of y -axis should be

$V(\mathbf{e}_{\bar{y}}) = \mathbf{e}_{\bar{y}}^T \mathbf{P} \mathbf{e}_{\bar{y}}$. The first derivative of $V(\mathbf{e}_{\bar{y}})$ is then can be defined as $\dot{V}(\mathbf{e}_{\bar{y}}) < 0$. The settling-time estimation error is then also fixed-time stable. In the next section, the disturbance observers for SSBM are presented.

Remark 7: The gains of fixed-time observers in Eqs. (48), (52), and (55) should approximately chose to avoid the chattering phenomenon.

B. THE DOB FOR SSBM SYSTEM

1) DOB FOR SPEED COORDINATE

The proposed DOB for estimating the perturbations on the speed coordinate is as follows:

$$\begin{aligned} \hat{T}_l &= -J \left(\frac{k_{nm}k_m A_m}{J} - \frac{\hat{T}_l}{J} + k_{1\omega} |e_\omega|^{\frac{\alpha_{1\omega}}{\beta_{1\omega}}} \text{sign}(e_\omega) \right. \\ &\quad \left. + k_{2\omega} |e_\omega|^{\frac{\alpha_{2\omega}}{\beta_{2\omega}}} \text{sign}(e_\omega) - \frac{k_{nm}k_m A_m}{J} \right) + k_{d\omega 1} \\ &\quad \times \int \left| -J \left(\frac{k_{nm}k_m A_m}{J} + k_{1\omega} |e_\omega|^{\frac{\alpha_{1\omega}}{\beta_{1\omega}}} \text{sign}(e_\omega) \right. \right. \\ &\quad \left. \left. + k_{2\omega} |e_\omega|^{\frac{\alpha_{2\omega}}{\beta_{2\omega}}} \text{sign}(e_\omega) - \frac{k_{nm}k_m A_m}{J} \right)^{\frac{1}{2}} \text{sign} \left(-J \left(\frac{k_{nm}k_m A_m}{J} \right. \right. \right. \\ &\quad \left. \left. + k_{1\omega} |e_\omega|^{\frac{\alpha_{1\omega}}{\beta_{1\omega}}} \text{sign}(e_\omega) + k_{2\omega} |e_\omega|^{\frac{\alpha_{2\omega}}{\beta_{2\omega}}} \text{sign}(e_\omega) - \frac{k_{nm}k_m A_m}{J} \right) \right) \\ &\quad \left. + k_{d\omega 2} \int \int \text{sign} \left(-J \left(\frac{k_{nm}k_m A_m}{J} + k_{1\omega} |e_\omega|^{\frac{\alpha_{1\omega}}{\beta_{1\omega}}} \text{sign}(e_\omega) \right. \right. \right. \right. \\ &\quad \left. \left. \left. + k_{2\omega} |e_\omega|^{\frac{\alpha_{2\omega}}{\beta_{2\omega}}} \text{sign}(e_\omega) - \frac{k_{nm}k_m A_m}{J} \right) \right) \right) \end{aligned} \quad (57)$$

where

$$\begin{cases} T_l = -J \left(\frac{k_{nm}k_m A_m}{J} - \frac{\hat{T}_l}{J} + k_{1\omega} |e_\omega|^{\frac{\alpha_{1\omega}}{\beta_{1\omega}}} \text{sign}(e_\omega) \right. \\ \quad \left. + k_{2\omega} |e_\omega|^{\frac{\alpha_{2\omega}}{\beta_{2\omega}}} \text{sign}(e_\omega) - \frac{k_{nm}k_m A_m}{J} \right) + k_{d\omega 1} \\ \tilde{T}_l = -J \left(\frac{k_{nm}k_m A_m}{J} + k_{1\omega} |e_\omega|^{\frac{\alpha_{1\omega}}{\beta_{1\omega}}} \text{sign}(e_\omega) \right. \\ \quad \left. + k_{2\omega} |e_\omega|^{\frac{\alpha_{2\omega}}{\beta_{2\omega}}} \text{sign}(e_\omega) - \frac{k_{nm}k_m A_m}{J} \right) + k_{d\omega 1} \end{cases} \quad (58)$$

According to the mentioned above, the proof of stability of the proposed DOB on speed coordinate was obtained. First, taking derivative for both sides of Eq. (57) yields

$$\dot{\hat{T}}_l = \dot{T}_l + k_{d\omega 1} |\tilde{T}_l|^{1/2} \text{sign}(\tilde{T}_l) + k_{d\omega 2} \int \text{sign}(\tilde{T}_l) \quad (59)$$

or

$$\dot{\hat{T}}_l = -k_{d\omega 1} |\tilde{T}_l|^{1/2} \text{sign}(\tilde{T}_l) - k_{d\omega 2} \int \text{sign}(\tilde{T}_l) \quad (60)$$

Similar as proof of the stability in Eqs. (37-39), Eq. (60) is called super-twisting DOB. The observer gains $k_{d\omega 1}$ and $k_{d\omega 2}$ must be positively defined.

2) DOB FOR MOVEMENT OF X-AXIS

The proposed DOB for movement of x -axis is shown as follows:

$$\hat{F}_{lx} = -m \left(\frac{k_{nb}k_b i_q}{m} - \frac{\hat{F}_{lx}}{m} + k_{2x} |x_1 - \hat{x}_1|^{\alpha_{2x}} \text{sign}(x_1 - \hat{x}_1) \right)$$

$$\begin{aligned}
 & -\frac{k_{nb}k_b i_q}{m}) + k_{d1x} \int \left| -m\left(\frac{k_{nb}k_b i_q}{m} + k_{2x} |x_1 - \hat{x}_1|^{\alpha_{2x}} \right. \right. \\
 & \times \left. \left. \text{sign}(x_1 - \hat{x}_1) - \frac{k_{nb}k_b i_q}{m} \right)^{1/2} \text{sign}\left(-m\left(\frac{k_{nb}k_b i_q}{m} \right. \right. \right. \\
 & \left. \left. \left. + k_{2x} |x_1 - \hat{x}_1|^{\alpha_{2x}} \text{sign}(x_1 - \hat{x}_1) - \frac{k_{nb}k_b i_q}{m} \right)\right) \right. \\
 & \left. + k_{d2x} \int \int \text{sign}\left(-m\left(\frac{k_{nb}k_b i_q}{m} - \frac{\hat{F}_{lx}}{m} + k_{2x} |x_1 - \hat{x}_1|^{\alpha_{2x}} \right. \right. \right. \\
 & \left. \left. \left. \times \text{sign}(x_1 - \hat{x}_1) - \frac{k_{nb}k_b i_q}{m} \right)\right) \right) \end{aligned} \quad (61)$$

where

$$\begin{cases} \hat{F}_{lx} = -m\left(\frac{k_{nb}k_b i_q}{m} - \frac{\hat{F}_{lx}}{m} + k_{2x} |x_1 - \hat{x}_1|^{\alpha_{2x}} \text{sign}(x_1 - \hat{x}_1) \right. \\ \left. - \frac{k_{nb}k_b i_q}{m} \right) \\ \tilde{F}_{lx} = -m\left(\frac{k_{nb}k_b i_q}{m} + k_{2x} |x_1 - \hat{x}_1|^{\alpha_{2x}} \text{sign}(x_1 - \hat{x}_1) \right. \\ \left. - \frac{k_{nb}k_b i_q}{m} \right) \end{cases} \quad (62)$$

Taking derivative for both sides of Eq. (61) leads

$$\dot{\hat{F}}_{lx} = \dot{F}_{lx} + k_{d1x} \left| \tilde{F}_{lx} \right|^{1/2} \text{sign}(\tilde{F}_{lx}) + k_{d2x} \int \text{sign}(\tilde{F}_{lx}) \quad (63)$$

or

$$\dot{\tilde{F}}_{lx} = -k_{d1x} \left| \tilde{F}_{lx} \right|^{1/2} \text{sign}(\tilde{F}_{lx}) - k_{d2x} \int \text{sign}(\tilde{F}_{lx}) \quad (64)$$

As the mentioned above, the observer gains k_{d1x} and k_{d2x} must be positively defined. Similarly, the proposed DOB for movement of y-axis is shown in the next following section.

3) DOB FOR MOVEMENT OF Y-AXIS

The proposed DOB for movement of y-axis is shown as follows:

$$\begin{aligned}
 \hat{F}_{ly} &= -m\left(\frac{k_{nb}k_b i_d}{m} - \frac{\hat{F}_{ly}}{m} + k_{2y} |y_1 - \hat{y}_1|^{\alpha_{2y}} \text{sign}(y_1 - \hat{y}_1) \right. \\
 & \left. - \frac{k_{nb}k_b i_d}{m} \right) + k_{d1y} \int \left| -m\left(\frac{k_{nb}k_b i_d}{m} + k_{2y} |y_1 - \hat{y}_1|^{\alpha_{2y}} \right. \right. \\
 & \times \left. \left. \text{sign}(y_1 - \hat{y}_1) - \frac{k_{nb}k_b i_d}{m} \right)^{1/2} \text{sign}\left(-m\left(\frac{k_{nb}k_b i_d}{m} \right. \right. \right. \\
 & \left. \left. \left. + k_{2y} |x_1 - \hat{x}_1|^{\alpha_{2x}} \text{sign}(x_1 - \hat{x}_1) - \frac{k_{nb}k_b i_q}{m} \right)\right) \right. \\
 & \left. + k_{d2y} \int \int \text{sign}\left(-m\left(\frac{k_{nb}k_b i_d}{m} - \frac{\hat{F}_{ly}}{m} + k_{2y} |y_1 - \hat{y}_1|^{\alpha_{2y}} \right. \right. \right. \\
 & \left. \left. \left. \times \text{sign}(y_1 - \hat{y}_1) - \frac{k_{nb}k_b i_d}{m} \right)\right) \right) \end{aligned} \quad (65)$$

where

$$\begin{cases} \hat{F}_{ly} = -m\left(\frac{k_{nb}k_b i_d}{m} - \frac{\hat{F}_{ly}}{m} + k_{2y} |y_1 - \hat{y}_1|^{\alpha_{2y}} \text{sign}(y_1 - \hat{y}_1) \right. \\ \left. - \frac{k_{nb}k_b i_d}{m} \right) \\ \tilde{F}_{ly} = -m\left(\frac{k_{nb}k_b i_d}{m} + k_{2y} |y_1 - \hat{y}_1|^{\alpha_{2y}} \text{sign}(y_1 - \hat{y}_1) \right. \\ \left. - \frac{k_{nb}k_b i_d}{m} \right) \end{cases} \quad (66)$$

Taking derivative for both sides of Eq. (66) leads

$$\dot{\hat{F}}_{ly} = \dot{F}_{ly} + k_{d1y} \left| \tilde{F}_{ly} \right|^{1/2} \text{sign}(\tilde{F}_{ly}) + k_{d2y} \int \text{sign}(\tilde{F}_{ly}) \quad (67)$$

or

$$\dot{\tilde{F}}_{ly} = -k_{d1y} \left| \tilde{F}_{ly} \right|^{1/2} \text{sign}(\tilde{F}_{ly}) - k_{d2y} \int \text{sign}(\tilde{F}_{ly}) \quad (68)$$

The observer gains k_{d1y} and k_{d2y} also must be positively defined. After obtained the information of the states and disturbances, the controllers for these movement operations are shown as follows:

C. FTSMC FOR SSBM SYSTEM

In this section, the variable boundary layer thickness FTSMC is introduced to control the speed of the rotational operation and positions of x- and y-axes, respectively.

1) FTSMC FOR SPEED AXIS

The sliding mode surface for speed control is as follows:

$$s_{\omega} = e_{\omega} + \lambda_{\omega} \int e_{\omega} \quad (69)$$

where $e_{\omega} = \omega_r - \hat{\omega}$. Taking the first derivative for both side of Eq. (69) yields

$$\dot{s}_{\omega} = \dot{e}_{\omega} + \lambda_{\omega} e_{\omega} \quad (70)$$

Using Eq. (48) to solve Eq. (70) leads to

$$\begin{aligned}
 \dot{s}_{\omega} &= \dot{\omega}_r - \frac{k_{nm}k_m A_m}{J} + \frac{\hat{T}_l}{J} - k_{1\omega} |e_{\omega}|^{\frac{\alpha_{1\omega}}{\beta_{1\omega}}} \text{sign}(e_{\omega}) \\
 & - k_{2\omega} |e_{\omega}|^{\frac{\alpha_{2\omega}}{\beta_{2\omega}}} \text{sign}(e_{\omega}) + \lambda_{\omega} e_{\omega} \end{aligned} \quad (71)$$

To obtain the equivalent control, \dot{s}_{ω} and estimated disturbance are considered equal to zero. There is a constant reference speed value. Therefore, $\dot{\omega}_r = 0$. The equivalent control input is then calculated as follows:

$$\begin{aligned}
 A_{meq} &= \frac{J}{k_{nm}k_m} (-k_{1\omega} |e_{\omega}|^{\frac{\alpha_{1\omega}}{\beta_{1\omega}}} \text{sign}(e_{\omega}) \\
 & - k_{2\omega} |e_{\omega}|^{\frac{\alpha_{2\omega}}{\beta_{2\omega}}} \text{sign}(e_{\omega})) + \lambda_{\omega} e_{\omega} \end{aligned} \quad (72)$$

The switching control was selected as follows:

$$A_{msw} = \frac{J}{k_{nm}k_m} (\gamma_{1\omega} |s_{\omega}|^{\frac{\kappa_{1\omega}}{\eta_{1\omega}}} \text{sat}\left(\frac{s_{\omega}}{\phi_{\omega}} - k_{0\omega} \int s_{\omega}\right)$$

$$+ \gamma_{2\omega} |s_\omega|^{\frac{\kappa 2\omega}{\eta 2\omega}} \text{sat}\left(\frac{s_\omega}{\phi_\omega} - k_{0\omega} \int s_\omega\right) \quad (73)$$

The stability of the control for speed axis is proved as below. First, the Lyapunov condition is selected as follows:

$$V(s_\omega) = \frac{1}{2} s_\omega^2 \quad (74)$$

Taking derivative for both sides of the Eq. (74) yields

$$\begin{aligned} \dot{V}(s_\omega) &= s_\omega \dot{s}_\omega \\ &= -s_\omega (\gamma_{1\omega} |s_\omega|^{\frac{\kappa 1\omega}{\eta 1\omega}} \text{sat}\left(\frac{s_\omega}{\phi_\omega} - k_{0\omega} \int s_\omega\right) \\ &\quad + \gamma_{2\omega} |s_\omega|^{\frac{\kappa 2\omega}{\eta 2\omega}} \text{sat}\left(\frac{s_\omega}{\phi_\omega} - k_{0\omega} \int s_\omega\right)) \\ &\leq 0 \end{aligned} \quad (75)$$

Proof:

Case 1: $\text{sat}\left(\frac{s_\omega}{\phi_\omega} - k_{0\omega} \int s_\omega\right) \in (-\phi_{\bar{\omega}}, \phi_{\bar{\omega}})$, Eq. (75) can be calculated as follows:

$$\dot{V}(s_\omega) = -s_\omega (\gamma_{1\omega} + \gamma_{2\omega}) \quad (76)$$

Taking integration for both sides of Eq. (76) corresponding to the time from zero to infinite yields

$$\int_0^{T_{\max}} \frac{d}{dt} \frac{V(s_\omega)}{s_\omega} d\tau = \int_0^{T_{\max}} -(\gamma_{1\omega} + \gamma_{2\omega}) d\tau \quad (77)$$

or

$$\int_0^{T_{\max}} \frac{d}{dt} s_\omega d\tau = \int_0^{T_{\max}} -(\gamma_{1\omega} + \gamma_{2\omega}) d\tau \quad (78)$$

or

$$T_{\max} \leq \frac{1}{(\gamma_{1\omega} + \gamma_{2\omega})} \quad (79)$$

Case 2: $\text{sat}\left(\frac{s_\omega}{\phi_\omega} - k_{0\omega} \int s_\omega\right) \notin (-\phi_{\bar{\omega}}, \phi_{\bar{\omega}})$, Eq. (75) can be calculated as below.

$$\begin{aligned} \dot{V}(s_\omega) &= -s_\omega (\gamma_{1\omega} |s_\omega|^{\frac{\kappa 1\omega}{\eta 1\omega}} \text{sign}(s_\omega) + \gamma_{2\omega} |s_\omega|^{\frac{\kappa 2\omega}{\eta 2\omega}} \\ &\quad \times \text{sign}(s_\omega)) \end{aligned} \quad (80)$$

According to the paper [28], the settling-time of Eq. (80) is calculated as follows:

$$T_{\max} \leq \frac{1}{\gamma_{1\omega}} \frac{\eta 1\omega}{\kappa 1\omega - \eta 1\omega} + \frac{1}{\gamma_{2\omega}} \frac{\eta 2\omega}{\eta 2\omega - \kappa 1\omega} \quad (81)$$

The settling-time of the speed control is fixed-time value.

2) FTSMC FOR X-AXIS

The sliding mode surface of x -axis is as follows:

$$s_{\bar{x}} = \dot{e}_{\bar{x}} + \lambda_{\bar{x}} e_{\bar{x}} \quad (82)$$

Taking the derivative for both sides of Eq. (82) yields

$$\dot{s}_{\bar{x}} = \ddot{e}_{\bar{x}} + \lambda_{\bar{x}} \dot{e}_{\bar{x}} \quad (83)$$

where $e_{\bar{x}} = x_r - \hat{x}$. Using Eq. (52) to solve Eq. (83) with the conditions of $\dot{s}_{\bar{x}} = 0$ and $\hat{F}_{lx} = 0$. The referenced input x_r is a constant value. Therefore, $\dot{x}_r = 0$.

$$-\frac{k_{nb} k_b i_q}{m} - k_{2x} |x_1 - \hat{x}_1|^{\alpha_{2x}} \text{sign}(x_1 - \hat{x}_1) + \lambda_{\bar{x}} \dot{e}_{\bar{x}} = 0 \quad (84)$$

The equivalent control value was calculated as follows:

$$i_{qeq} = \frac{m}{k_{nb} k_b} [-k_{2x} |x_1 - \hat{x}_1|^{\alpha_{2x}} \text{sign}(x_1 - \hat{x}_1) + \lambda_{\bar{x}} \dot{e}_{\bar{x}}] \quad (85)$$

The switching control was designed as follows:

$$\begin{aligned} i_{qsw} &= \gamma_{1\bar{x}} |s_{\bar{x}}|^{\frac{\kappa 1\bar{x}}{\eta 1\bar{x}}} \text{sat}\left(\frac{s_{\bar{x}}}{\phi_{\bar{x}}} - k_{0\bar{x}} \int s_{\bar{x}}\right) + \gamma_{2\bar{x}} |s_{\bar{x}}|^{\frac{\kappa 2\bar{x}}{\eta 2\bar{x}}} \\ &\quad \times \text{sat}\left(\frac{s_{\bar{x}}}{\phi_{\bar{x}}} - k_{0\bar{x}} \int s_{\bar{x}}\right) \end{aligned} \quad (86)$$

Similar as the proof of Eqs. (74-75), the $V(s_{\bar{x}}) = 0.5 s_{\bar{x}}^2 \geq 0$, the first derivative $\dot{V}(s_{\bar{x}}) \leq 0$. The settling-time is then also fixed-time stable. Similarly, the control of the movement on y -axis is designed as the next following section below.

Remark 8: The stabilities of the proposed controls for position on x -axis and y -axis can be proved as the same of poof of stability analysis for speed control in Eqs. (76) to (81).

3) FTSMC FOR Y-AXIS

The sliding mode surface of x -axis control is as follows:

$$s_{\bar{y}} = \dot{e}_{\bar{y}} + \lambda_{\bar{y}} e_{\bar{y}} \quad (87)$$

Taking the derivative for both sides of Eq. (87) yields

$$\dot{s}_{\bar{y}} = \ddot{e}_{\bar{y}} + \lambda_{\bar{y}} \dot{e}_{\bar{y}} \quad (88)$$

where $e_{\bar{y}} = y_r - \hat{y}$. Using Eq. (55) to solve Eq. (88) with the conditions of $\dot{s}_{\bar{y}} = 0$ and $\hat{F}_{ly} = 0$. The referenced input y_r is a constant value. Therefore, $\dot{y}_r = 0$.

$$-\frac{k_{nb} k_b i_d}{m} - k_{2y} |y_1 - \hat{y}_1|^{\alpha_{2y}} \text{sign}(y_1 - \hat{y}_1) + \lambda_{\bar{y}} \dot{e}_{\bar{y}} = 0 \quad (89)$$

The equivalent control value was calculated as follows:

$$i_{deq} = \frac{m}{k_{nb} k_b} [-k_{2y} |y_1 - \hat{y}_1|^{\alpha_{2y}} \text{sign}(y_1 - \hat{y}_1) + \lambda_{\bar{y}} \dot{e}_{\bar{y}}] \quad (90)$$

The switching control was designed as follows:

$$\begin{aligned} i_{dsw} &= \gamma_{1\bar{y}} |s_{\bar{y}}|^{\frac{\kappa 1\bar{y}}{\eta 1\bar{y}}} \text{sat}\left(\frac{s_{\bar{y}}}{\phi_{\bar{y}}} - k_{0\bar{y}} \int s_{\bar{y}}\right) + \gamma_{2\bar{y}} |s_{\bar{y}}|^{\frac{\kappa 2\bar{y}}{\eta 2\bar{y}}} \\ &\quad \times \text{sat}\left(\frac{s_{\bar{y}}}{\phi_{\bar{y}}} - k_{0\bar{y}} \int s_{\bar{y}}\right) \end{aligned} \quad (91)$$

Similar as the proof of Eqs. (74-75), the $V(s_{\bar{y}}) = 0.5 s_{\bar{y}}^2 \geq 0$, the first derivative $\dot{V}(s_{\bar{y}}) \leq 0$. The settling-time is also fixed-time stable. The stability of the proposed algorithms for the SSBM is proved as the next section below.

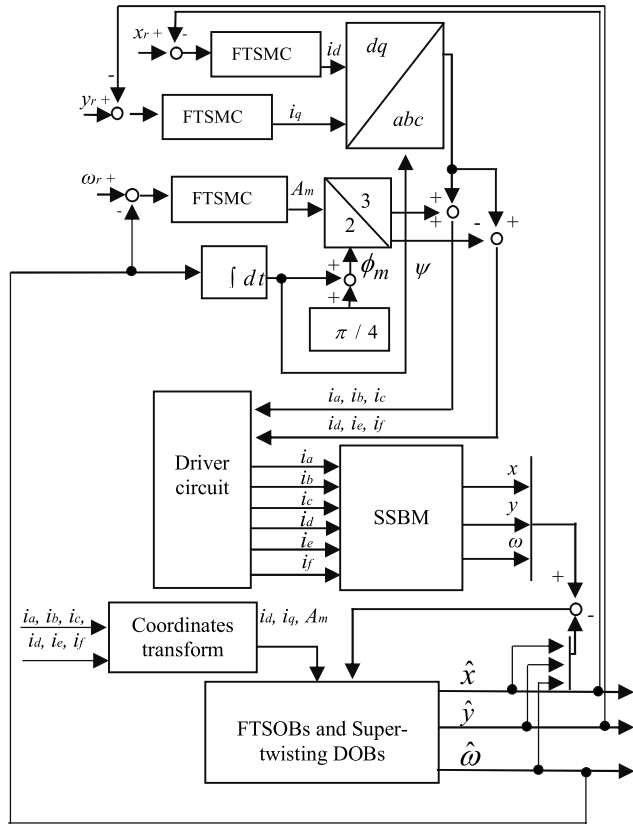


FIGURE 2. Control system of SSBM.

Stability Analysis: The Luapunov condition is selected as follows:

$$V(s_{total}) = \frac{1}{2}s_{\tilde{x}}^2 + \frac{1}{2}s_{\tilde{y}}^2 + \frac{1}{2}s_{\tilde{\omega}}^2 + \frac{1}{2}\tilde{T}_l^2 + \frac{1}{2}\tilde{F}_{lx}^2 + \frac{1}{2}\tilde{F}_{ly}^2 + V(e_{\omega}) + V(e_{\tilde{x}}) + V(e_{\tilde{y}}) \quad (92)$$

Taking the first derivative for both sides of Eq. (92) yields

$$\dot{V}(s_{total}) = s_{\tilde{x}}\dot{s}_{\tilde{x}} + s_{\tilde{y}}\dot{s}_{\tilde{y}} + s_{\tilde{\omega}}\dot{s}_{\tilde{\omega}} + \tilde{T}_l\dot{\tilde{T}}_l + \tilde{F}_{lx}\dot{\tilde{F}}_{lx} + \tilde{F}_{ly}\dot{\tilde{F}}_{ly} + \dot{V}(e_{\omega}) + \dot{V}(e_{\tilde{x}}) + \dot{V}(e_{\tilde{y}}) \quad (93)$$

From section (3.1), Eqs. (60), (62), (66), (83-86), and (88-90), Eq. (93) can be defined as a negative value as follows:

$$\dot{V}(s_{total}) < 0 \quad (94)$$

This completes the proof of the stability.

Remark 9: The stability of the whole control system is finite time due to disturbance observer errors are finite time.

The performance of the proposed methods are shown in the next following section below.

IV. AN ILLUSTRATIVE EXAMPLE

In this section, the simulation of the proposed control algorithms is given with the comparison of the performances of the proposed methods and the existing method such as in [10]. The tested disturbances were used for same SSBM of this paper and the previous one [10] to show the superior performance of the proposed control algorithm. Herein, the control

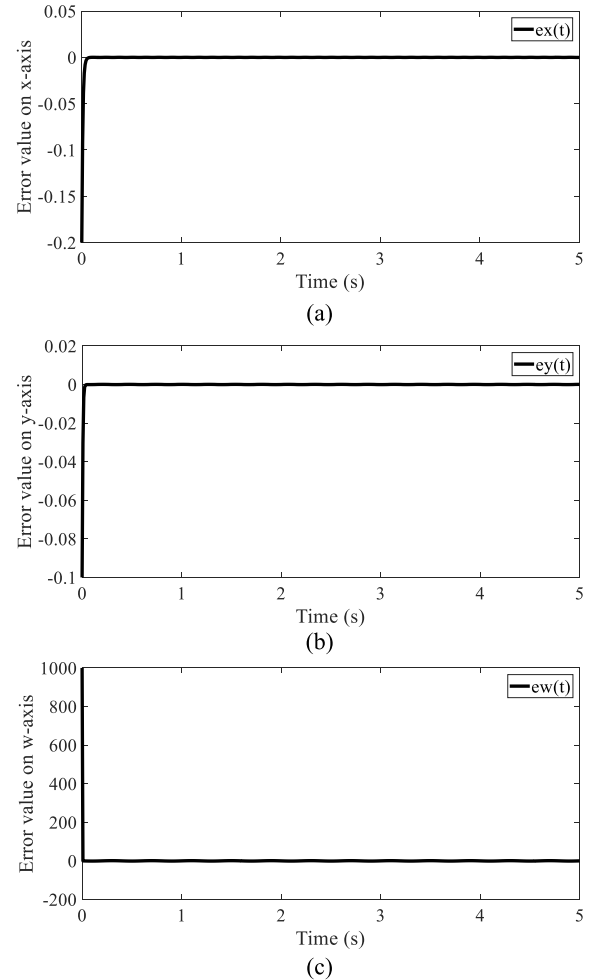


FIGURE 3. The error of positions and speed control: (a) position error on x-axis, (b) position error on y-axis, (c) position error on ω -axis.

values of the proposed control algorithms were used to control the SSBM through the driver circuit as Figure 2 below. The control inputs on all phases need to be measured and converted to the direct, quadrature, and motor current axes, respectively. The estimated states were used to design the controllers for three movement operations. The structure of the proposed control algorithms for SSBM is shown as in the Figure. 2 below.

The control parameters are as follows: First the disturbance observer gains are positively defined as follows: The gains of the DOB for position axes should be suitable small as $k_{dx1} = 80, k_{dx2} = 70, k_{dy1} = 35, k_{dy2} = 100$, and the gains of DOB for speed axis should large enough due to the coefficient J is very small. These gains were chosen as follows $k_{d\omega 1} = 2 \cdot 10^5$ and $k_{d\omega 2} = 1 \cdot 10^5$. The gains of the state observers were suitably selected to avoid the chattering values such as follows: $k_{1\omega} = 2000, k_{2\omega} = 2500, k_{1x} = 100, k_{2x} = 5000, k_{1y} = 20, k_{2y} = 7500$. The order fixed-time observer for speed axis should be chosen to fulfil the condition of fixed-time stability of Eq. (42). These values were selected as follows: $\alpha_{1\omega} = 6, \beta_{1\omega} = 5, \alpha_{2\omega} = 3$, and $\beta_{2\omega} = 4$. The order of the observers for x - and y -axes

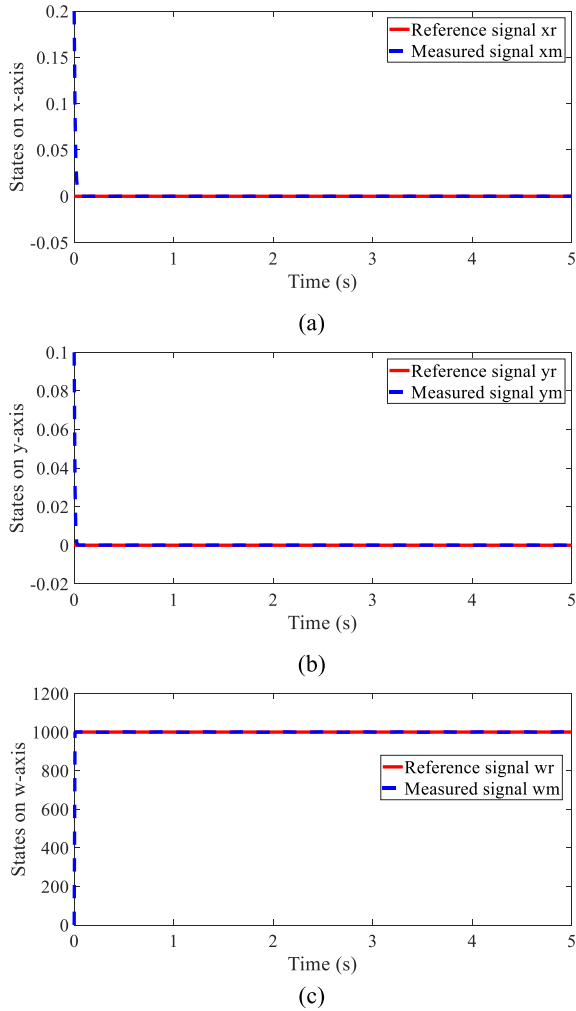


FIGURE 4. Referenced and measured states: (a) signals of x-axis, (b) signals of y-axis, and (c) signals of ω -axis.

should be chosen as $\alpha_{1x} = 0.85$, $\alpha_{2x} = 0.7$, $\alpha_{1y} = 0.85$, and $\alpha_{2y} = 0.7$ to satisfy the constraint as proof form Eqs 23-30. The parameters of sliding surface were positively defined as follows: $\lambda_{\tilde{x}} = 125$, $\lambda_{\tilde{y}} = 200$, and $\lambda_{\tilde{\omega}} = 1$. The control gains were suitably selected as follows: $\gamma_{1\tilde{x}} = 50$, $\gamma_{2\tilde{x}} = 75$, $\gamma_{1\tilde{y}} = 75$, $\gamma_{2\tilde{y}} = 300$, $\gamma_{1\tilde{\omega}} = 0.0125$, and $\gamma_{2\tilde{\omega}} = 0.015$. The order fixed-time controller were suitably selected as follows: $\kappa_1\tilde{x} = 7$, $\eta_1\tilde{x} = 4$, $\kappa_2\tilde{x} = 3$, $\eta_2\tilde{x} = 4$, $\kappa_1\tilde{y} = 3$, $\eta_1\tilde{y} = 2$, $\kappa_2\tilde{y} = 3$, $\eta_1\tilde{y} = 4$, $\kappa_1\tilde{y} = 6$, $\eta_1\tilde{y} = 5$, $\kappa_1\tilde{\omega} = 3$, and $\kappa_1\tilde{\omega} = 4$. The boundary layer thicknesses and adaptive gains were selected small enough as follows: $\phi_{\tilde{x}} = 0.02$, $k_{0\tilde{x}} = 0.125$, $\phi_{\tilde{y}} = 0.01$, $k_{0\tilde{y}} = 0.125$, $\phi_{\tilde{\omega}} = 0.01$, $k_{0\tilde{\omega}} = 0.125$. The tested disturbances and uncertainties are as follows: $F_{lx} = 1.25 \sin(15\pi t)$, $F_{ly} = 1.5 \sin(7.5\pi t)$, and $\hat{T}_l = 0.1 \sin(5\pi t)$ for x -, y -, and ω -axes, respectively. The performances of the proposed control algorithms for SSBM with the case of the disturbances on three axes is as in the Figures. 3-6 below.

The settling-times for control of x -, y -, and ω -axes are about $T_{ex} < 0.1(s)$, $T_{ey} < 0.06 (s)$, and $T_{e\omega} < 0.01$, respectively. The overshoots for these axes are

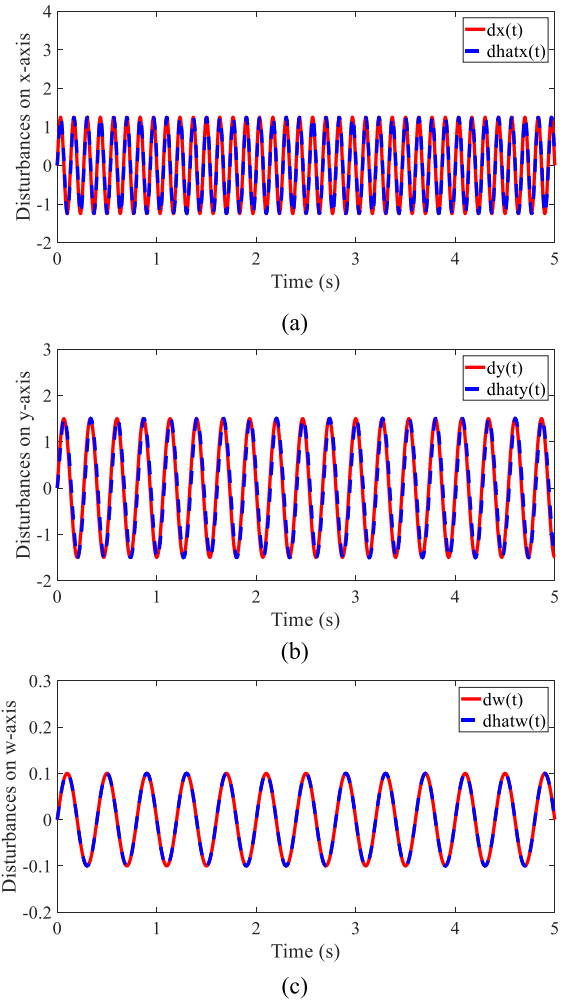


FIGURE 5. Tested and estimated disturbances: (a) disturbances on x-axis, (b) disturbances on y-axis, and (c) disturbances on ω -axis.

$O_{ex} < 6.7 \times 10^{-5} (mm)$, $O_{ey} < 5.4 \times 10^{-5} (mm)$, and $O_{e\omega} < 0.5 (rad/s)$, respectively. The steady-states of these axes are $e_x \in (-7, 7) \times 10^{-5} (mm)$, $e_y \in (-5.8, 5.8) \times 10^{-5} (mm)$ and $e_\omega \in (-1, 1) (rad/s)$. The performances of the proposed control algorithms with the fully tested disturbances on three axes were very good. The output signals of the three movements on three axes are shown in Figure 4 below.

The measured and referenced signals were mostly identical. The disturbances were tested on three axes are time-varying with low and high frequency values. The main effort of using the different time-varying disturbances is aimed to confirm that the proposed disturbance observer is good at rejecting the disturbance and uncertainty for the SSBM system at any frequencies. In fact, the time-varying disturbance is changing problem to many DOB with the conjunction of the first derivative equal to zero. The performances of our proposed disturbance observer are shown as the Figure 5 below.

As shown in Figure 5 above, the tested and estimated disturbances were mostly identical. These values were tracked each other in an acceptably short time period. Both low and

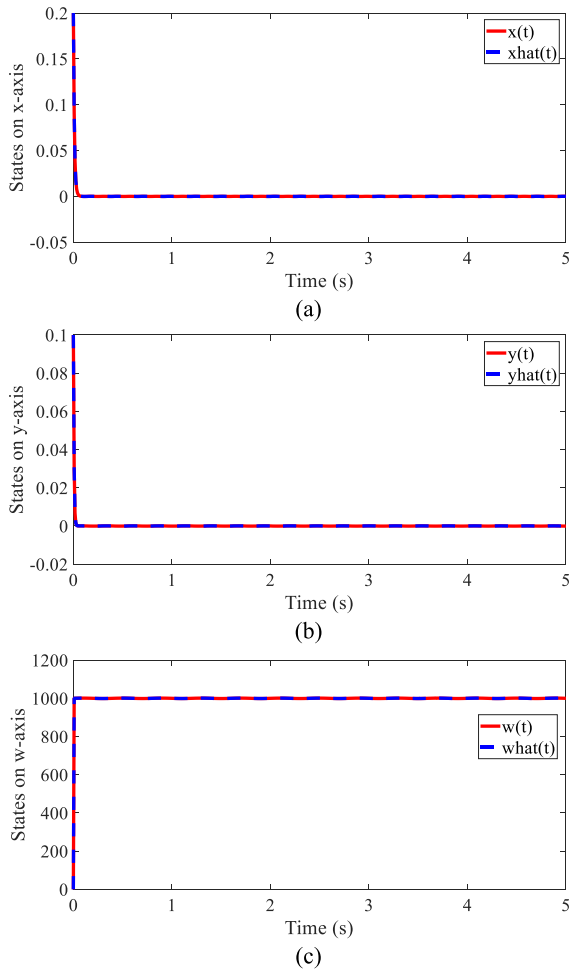


FIGURE 6. Measured and estimated states of the SSBM: (a) states on x-axis, (b) states on y-axis, and (c) states on ω -axis.

high frequencies of disturbance values were all estimated and rejected by the proposed DOB. There is new DOB also used information of measured and estimated states [33], [34]. However, the proposed DOB in this paper was directly constructed with the relation of disturbance error and its functions. In [33], the estimated disturbance information was designed with information of state errors and estimated disturbance information. In [34], the first derivative disturbance still need to be bounded. However, the proposed methods is mainly focused for estimate the states and reject the partially unknown dynamic due to the expectation of the mathematical model of SSBM as shown in Eq. (18). That is the reason of difference between this work and some previous papers [35], [36]. Furthermore, to show the effectiveness of the fixed-time state observer, the measured and estimated states of the SSBM are shown in Figure 6 below.

The initial states of the real and observed systems were defined identical as $x(0) = \hat{x}(0) = 0.2$ (mm), $y(0) = \hat{y}(0) = 0.1$ (mm) and $\omega(0) = \hat{\omega}(0) = 0$ (V). The performances in Figure 6 defines that the state observer was good at estimating real state of the SSBM system. To show the superior performance of the proposed DOB of this paper, the comparison of the proposed method in [10] and this work is given. The same

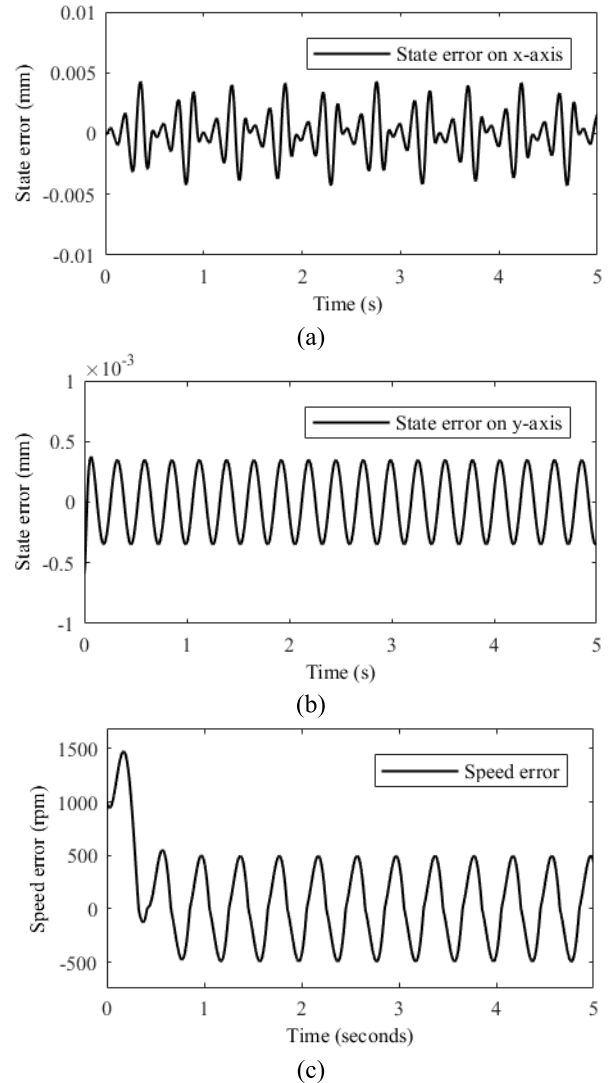


FIGURE 7. State errors: (a) error on x-axis, (b) error on y-axis, and (c) error on ω -axis.

disturbances on x - and ω -axes are $F_{lx} = 1.25 \sin(15\pi t)$, and $\hat{T}_l = 0.1 \sin(5\pi t)$, respectively. The tested disturbance for y -axis same with it in the Figure 5b for proposed method in [10] leads performance on y -axis to divergence. Therefore, the tested disturbance for controller in [10] is reduced by $F_{ly} = 1.0 \sin(7.5\pi t)$. The performances of the proposed method in [10] with tested disturbance above are shown as the Figure 7 below.

The state errors for three axes are quite big in compare with the performances of our proposed method. Furthermore, the comparison of the performances of the proposed method with tested disturbances and the control method in [10] without the tested disturbances are shown in the Table 1 below.

The comparison of this paper and previous paper was shown that the proposed control algorithms of this paper is robustness. The proposed disturbance observer was very effective with the time-varying disturbance at any frequencies.

TABLE 1. Comparison of the proposed method with paper [10].

Values	THIS PAPER RESULTS	PREVIOUS PAPER [10]
Overshoots	$O_{ex} < 6.7 \times 10^{-5}$ (mm),	$O_{ex} \gg 6.7 \times 10^{-5}$ (mm),
	$O_{ey} < 5.4 \times 10^{-5}$ (mm), and $O_{e\omega} < 0.5$ (rad/s).	$O_{ey} > 0.2$ (mm), and $O_{e\omega}$ did not clearly shown.
Settling-times	$T_{ex} < 0.1$ (s),	$T_{ex} > 0.1$ (s), $T_{ey} > 0.1$
	$T_{ey} < 0.06$ (s), and $T_{e\omega} < 0.01$ (s)	(s), and $T_{e\omega} > 2$ (s)
States error	$e_x \in (-7, 7) \times 10^{-5}$ (mm),	Did not shown, but more unstable than the performances of this paper.
	$e_y \in (-5.8, 5.8) \times 10^{-5}$ (mm), $e_{\omega} \in (-1, 1)$ (rad/s).	
Disturbance rejection ability	Yes	No

V. CONCLUSION

This paper proposed a new super-twisting DOB for estimating the disturbances and uncertainties of the outside effects and inside parameter variations of the SSBM system. The perturbations of SSBM were obtained based on the information of the estimated and measured states. The condition of the first derivative disturbance equal to zero is here free. The disturbance errors converges to zero in finite-times with the fast speed and stable of a super-twisting functions. This is also one of the originality of the paper. Furthermore, the fixed-time state observer concept was used to design the state observer for the speed coordinate and the homogenous fixed-time stability was used to design the state observer for the movement on x - and y -axes, respectively. After obtained the information of the disturbances and system states, the variable boundary layer thickness FTSMC was designed for controlling the position on x - and y -axes and rotational speed on ω -axis, respectively. The obtained results shown that the proposed control algorithms are good for SSBM. The tested disturbances were mostly rejected by the proposed super-twisting DOB, the system states were precisely obtained by the proposed fixed-time state observer. Furthermore, the positions and speed control was good at forcing the rotor stable in predefined position and the desired speed, respectively. In the next study, a new DOB with the basic design of estimated and measured states in this paper will be proposed to improve the settling-time of disturbance error. Furthermore, the state observer will be improved to obtain the states of SSBM in short time and without the chattering of switching function.

REFERENCES

- [1] V.-N. Giap and S.-C. Huang, "Effectiveness of fuzzy sliding mode control boundary layer based on uncertainty and disturbance compensator on suspension active magnetic bearing system," *Meas. Control*, vol. 53, nos. 5–6, pp. 934–942, Mar. 2020.
- [2] V. N. Giap and S. C. Huang, "Generalized proportional integral disturbance observer-based fuzzy sliding mode control for active magnetic bearing system," *IOP Conf. Ser., Mater. Sci. Eng.*, vol. 1113, no. 1, Mar. 2021, Art. no. 012006.
- [3] V. N. Giap, S.-C. Huang, Q. D. Nguyen, and X. T. Trinh, "Time varying disturbance observer based on sliding mode control for active magnetic bearing system," in *Proc. Int. Conf. Mater., Mach. Methods Sustain. Develop.*, 2020, pp. 929–935.
- [4] T.-J. Su, W.-P. Kuo, V.-N. Giap, H. Q. Vu, and Q.-D. Nguyen, "Active magnetic bearing system using PID-surface sliding mode control," in *Proc. 3rd Int. Conf. Comput. Meas. Control Sensor Netw. (CMCSN)*, May 2016, pp. 5–8, doi: 10.1109/CMCSN.2016.31.
- [5] J. S. H. Tsai, T. J. Su, J.-C. Cheng, Y.-Y. Lin, V.-N. Giap, S. M. Guo, and L. S. Shieh, "Robust observer-based optimal linear quadratic tracker for five-degree-of-freedom sampled-data active magnetic bearing system," *Int. J. Syst. Sci.*, vol. 49, no. 6, pp. 1273–1299, Apr. 2018.
- [6] D. Steinert, T. Nussbaumer, and J. W. Kolar, "Slotless bearingless disk drive for high-speed and high-purity applications," *IEEE Trans. Power Electron.*, vol. 61, no. 11, pp. 5974–5986, Nov. 2014.
- [7] D. Steinert, T. Nussbaumer, and J. W. Kolar, "Evaluation of one- and two-pole-pair slotless bearingless motors with toroidal windings," *IEEE Trans. Ind. Appl.*, vol. 52, no. 1, pp. 172–180, Jan. 2016.
- [8] S. Ueno, S.-I. Uematsu, and T. Kato, "Development of a lorentz-force-type slotless self-bearing motor," *J. Syst. Des. Dyn.*, vol. 3, no. 4, pp. 462–470, 2009.
- [9] S. Ueno and T. Kato, "A novel design of a Lorentz-force-type small self-bearing motor," in *Proc. 8th Int. Conf. Power Electron. Drive Syst. (PEDS)*, Nov. 2009, pp. 926–931.
- [10] H. P. Nguyen, X. B. Nguyen, T. T. Bui, S. Ueno, and Q. D. Nguyen, "Analysis and control of slotless self-bearing motor," *Actuators*, vol. 8, no. 3, pp. 1–17, 2019.
- [11] Q. D. Nguyen and S. Ueno, "Analysis and control of nonsalient permanent magnet axial gap self-bearing motor," *IEEE Trans. Ind. Electron.*, vol. 58, no. 7, pp. 2644–2652, Jul. 2011.
- [12] Q. D. Nguyen and S. Ueno, "Modeling and control of salient-pole permanent magnet axial-gap self-bearing motor," *IEEE/ASME Trans. Mechatronics*, vol. 16, no. 3, pp. 518–526, Jun. 2011.
- [13] B. Sarsembayev, K. Suleimenov, and T. D. Do, "High order disturbance observer based PI-PI control system with tracking anti-windup technique for improvement of transient performance of PMSM," *IEEE Access*, vol. 9, pp. 66323–66334, 2021.
- [14] V.-P. Vu, V.-T. Ngo, V.-D. Do, D.-N. Truong, T.-T. Huynh, and T. D. Do, "Robust MPPT observer-based control system for wind energy conversion system with uncertainties and disturbance," *IEEE Access*, vol. 9, pp. 96466–96477, 2021, doi: 10.1109/ACCESS.2021.3094819.
- [15] V.-P. Vu and T. D. Do, "Fault/state estimation observer synthesis for uncertain T-S fuzzy systems," *IEEE Access*, vol. 7, pp. 358–369, 2019, doi: 10.1109/ACCESS.2018.2885379.
- [16] W.-H. Chen, D. J. Ballance, P. J. Gawthrop, and J. O'Reilly, "A nonlinear disturbance observer for robotic manipulators," *IEEE Trans. Ind. Electron.*, vol. 47, no. 4, pp. 932–938, Aug. 2000, doi: 10.1109/41.857974.
- [17] A. T. Nguyen, B. A. Basit, H. H. Choi, and J.-W. Jung, "Disturbance attenuation for surface-mounted PMSM drives using nonlinear disturbance observer-based sliding mode control," *IEEE Access*, vol. 8, pp. 86345–86356, 2020.
- [18] X. Wu, K. Xu, M. Lei, and X. He, "Disturbance-compensation-based continuous sliding mode control for overhead cranes with disturbances," *IEEE Trans. Autom. Sci. Eng.*, vol. 17, no. 4, pp. 2182–2189, Oct. 2020.
- [19] V. N. Giap, S.-C. Huang, Q. D. Nguyen, and T.-J. Su, "Disturbance observer-based linear matrix inequality for the synchronization of Takagi–Sugeno fuzzy chaotic systems," *IEEE Access*, vol. 8, pp. 225805–225821, 2020.
- [20] V. N. Giap, Q. D. Nguyen, and S. C. Huang, "Synthetic adaptive fuzzy disturbance observer and sliding-mode control for chaos-based secure communication systems," *IEEE Access*, vol. 9, pp. 23907–23928, 2021.
- [21] N. V. Giap, H. S. Vu, Q. D. Nguyen, and S.-C. Huang, "Disturbance and uncertainty rejection-based on fixed-time sliding-mode control for the secure communication of chaotic systems," *IEEE Access*, vol. 9, pp. 133663–133685, 2021.
- [22] V.-N. Giap, S.-C. Huang, Q. D. Nguyen, and T.-J. Su, "Robust control-based disturbance observer and optimal states feedback for T-S fuzzy systems," *J. Low Freq. Noise, Vib. Act. Control*, vol. 40, no. 3, pp. 1509–1525, Dec. 2020.
- [23] V. N. Giap, H.-S. Vu, Q. D. Nguyen, and S.-C. Huang, "Robust observer based on fixed-time sliding mode control of position/velocity for a T-S fuzzy MEMS gyroscope," *IEEE Access*, vol. 9, pp. 96390–96403, 2021, doi: 10.1109/ACCESS.2021.3095465.

- [24] S. Hwang and H. S. Kim, "Extended disturbance observer-based integral sliding mode control for nonlinear system via T-S fuzzy model," *IEEE Access*, vol. 8, pp. 116090–116105, 2020.
- [25] M. Basin, P. Yu, and Y. Shtessel, "Finite- and fixed-time differentiators utilising HOSM techniques," *IET Control Theory Appl.*, vol. 11, no. 8, pp. 1144–1152, May 2017.
- [26] V. Utkin, "Variable structure systems with sliding modes," *IEEE Trans. Autom. Control*, vol. 22, no. 2, pp. 212–222, Apr. 1997.
- [27] C.-C. Fuh, "Variable-thickness boundary layers for sliding mode control," *J. Mar. Sci. Technol.*, vol. 16, no. 4, pp. 288–294, 2008.
- [28] A. Polyakov, "Nonlinear feedback design for fixed-time stabilization of linear control systems," *IEEE Trans. Autom. Control*, vol. 57, no. 8, pp. 2106–2110, Aug. 2012.
- [29] H. Li and Y. Cai, "On SFTSM control with fixed-time convergence," *IET Control Theory Appl.*, vol. 11, no. 6, pp. 766–773, Apr. 2017.
- [30] Y. Tian, Y. Cai, and Y. Deng, "A fast nonsingular terminal sliding mode control method for nonlinear systems with fixed-time stability guarantees," *IEEE Access*, vol. 8, pp. 60444–60454, 2020.
- [31] L. Wang, H. Du, W. Zhang, D. Wu, and W. Zhu, "Implementation of integral fixed-time sliding mode controller for speed regulation of PMSM servo system," *Nonlinear Dyn.*, vol. 102, no. 1, pp. 185–196, Sep. 2020.
- [32] S. Wu, X. Su, and K. Wang, "Time-dependent global nonsingular fixed-time terminal sliding mode control-based speed tracking of permanent magnet synchronous motor," *IEEE Access*, vol. 8, pp. 186408–186420, 2020.
- [33] X. Bu, X. Wu, R. Zhang, Z. Ma, and J. Huang, "Tracking differentiator design for the robust backstepping control of a flexible air-breathing hypersonic vehicle," *J. Franklin Inst.*, vol. 352, no. 4, pp. 1739–1765, Apr. 2015.
- [34] X. Bu, D. Wei, and G. He, "A robust constrained control approach for flexible air-breathing hypersonic vehicles," *Int. J. Robust Nonlinear Control*, vol. 30, no. 7, pp. 2752–2776, May 2020.
- [35] X. Bu and Q. Qi, "Fuzzy optimal tracking control of hypersonic flight vehicles via single-network adaptive critic design," *IEEE Trans. Fuzzy Syst.*, vol. 30, no. 1, pp. 270–278, Jan. 2022, doi: [10.1109/TFUZZ.2020.3036706](https://doi.org/10.1109/TFUZZ.2020.3036706).
- [36] X. Bu, Q. Qi, and B. Jiang, "A simplified finite-time fuzzy neural controller with prescribed performance applied to waverider aircraft," *IEEE Trans. Fuzzy Syst.*, early access, Jun. 14, 2021, doi: [10.1109/TFUZZ.2021.3089031](https://doi.org/10.1109/TFUZZ.2021.3089031).



QUANG DICH NGUYEN received the B.S. degree in electrical engineering from the Hanoi University of Technology, Hanoi, Vietnam, in 1997, the M.S. degree in electrical engineering from the Dresden University of Technology, Dresden, Germany, in 2003, and the Ph.D. degree from Ritsumeikan University, Kusatsu, Japan, in 2010. Since 2000, he has been with the Hanoi University of Science and Technology, where he is currently an Associate Professor and an Executive Dean of the Institute for Control Engineering and Automation. His research interests include magnetic bearings, self-bearing motors, and sensorless motor control.



HUY PHUONG NGUYEN was born in Hanoi, Vietnam. He received the Engineering and Ph.D. degrees in industry automation from the Moscow Power Engineering Institute, Russia, in 1997 and 2000, respectively. Since 2002, he has been joined the Department of Industrial Automation and is currently an Associate Professor with the School of Electrical Engineering, Hanoi University of Science and Technology. His research interests include power plant process, process control in industry, motor control, and automation.



DUC NHAN VO was born in Binh Dinh, Vietnam. He received the Engineering and master's degrees in electrical engineering from the Da Nang University of Science and Technology, Vietnam, in 2007 and 2012, respectively. He is currently pursuing the Ph.D. degree with the Institute for Control Engineering and Automation, Hanoi University of Science and Technology. His research interests include self-bearing motor, magnetic bearing, and slotless motor.



XUAN BIEN NGUYEN received the B.S. and master's degrees in control engineering and automation from the Hanoi University of Science and Technology, Hanoi, Vietnam, in 2019 and 2020, respectively. He is currently working at Thuy-loi University and Hanoi University of Science and Technology. His research interests include the magnetic bearing systems, slotless self-bearing motors, sliding mode control, and motor control.



SATOSHI UENO (Senior Member, IEEE) received the B.S.M.E., M.S.M.E., and D.Eng. degrees from Ibaraki University, Hitachi, Japan, in 1995, 1997, and 2000, respectively. From 2000 to 2004, he was a Research Associate with the Department of Intelligent Machines and System Engineering, Hirosaki University, Hirosaki, Japan. He is currently a Professor in mechanical engineering with Ritsumeikan University, Kusatsu, Japan. His research interests include active magnetic bearings, self-bearing motors, and their applications. He is a member of the Japan Society of Mechanical Engineers, Institute of Electric Engineers of Japan, and several other societies.



SHYH-CHOUR HUANG (Senior Member, IEEE) received the bachelor's degree in aeronautics and astronautics engineering from the National Cheng-Kung University, in 1980, Taiwan, and the Ph.D. degree in mechanical engineering from the University of Cincinnati, USA, in 1990. He is currently a Professor in mechanical engineering with the National Kaohsiung University of Science and Technology, Taiwan. His research interests include micro-electromechanical systems design, biomechanics, compliant mechanisms, multibody dynamics, fuzzy logic control, vibration control, and optimization algorithms.



VAN NAM GIAP received the B.S. degree in control engineering and automation from the Hanoi University of Science and Technology, Hanoi, Vietnam, in 2015, the master's degree in electronic engineering from the National Kaohsiung University of Applied and Sciences, Kaohsiung, Taiwan, in 2017, and the Ph.D. degree in mechanical engineering from the National Kaohsiung University of Science and Technology, Taiwan, in June 2021. He is currently with the Hanoi University of Science and Technology. His research interests include sliding mode control, disturbance and uncertainty estimation, fuzzy logic control, secure communication, the magnetic bearing system and its applications, and self-bearing motors.

• • •